Signal Processing 90 (2010) 2965–2980

Contents lists available at ScienceDirect

Signal Processing

journal homepage: www.elsevier.com/locate/sigpro

MIMO OFDM systems with digital RF impairment compensation

Deepaknath Tandur *,♣, Marc Moonen ♣

Katholieke Universiteit Leuven-ESAT/SCD-SISTA, Kasteelpark Arenberg 10, B-3001 Leuven, Belgium

ARTICLE INFO

Article history:
Received 5 August 2009
Received in revised form
18 February 2010
Accepted 27 April 2010
Available online 8 May 2010

Keywords:
IQ imbalance
CFO
Direct conversion front-end
OFDM
MIMO

ABSTRACT

Multi-input multi-output (MIMO) systems are often realized with low cost front-end architectures, e.g. the so-called direct conversion (or zero IF) architectures. However, such systems are very sensitive to imperfections in the analog front-end resulting in radio frequency (RF) impairments such as in-phase/quadrature-phase (IQ) imbalance and carrier frequency offset (CFO). These RF impairments can result in a severe performance degradation. In this paper we propose RF impairment compensation techniques for orthogonal frequency division multiplexing (OFDM) based MIMO systems. We consider a digital compensation scheme for joint transmitter/receiver frequency selective IQ imbalance, CFO and channel distortion. We also show that in the case where there is no transmitter IQ imbalance, the receiver IQ imbalance compensation can be de-coupled from the channel equalization resulting in a compensation in two stages. The two-stage scheme results in an overall lower computational requirement. The various compensation schemes are demonstrated to provide a performance close to the ideal case without RF impairments.

© 2010 Elsevier B.V. All rights reserved.

1. Introduction

Orthogonal frequency division multiplexing (OFDM) is a widely adopted modulation technique for broadband communication systems [1]. It has been standardized for a variety of applications, such as wireless local area networks (WLANs), digital audio broadcasting (DAB), digital video broadcasting (DVB-T) and asymmetric digital subscriber lines (ADSLs), etc.

OFDM has also become a preferred modulation format in multiple antenna based transmission systems [2]. An OFDM based so-called multi-input multi-output (MIMO) transmission system takes advantage of the spatial diversity obtained by its multiple transmit and receive antennas to improve its performance in a dense multipath fading environment. As the MIMO OFDM architecture has to support multiple parallel front-end radios, it is extremely important to keep these radio frequency (RF) front-ends simple with minimal analog electronics so as to maintain the cost, size and power consumption within an acceptable limit.

The so-called direct conversion (or zero IF) architecture provides a good implementation alternative for such systems compared to the traditional superheterodyne front-end architecture [3]. The direct conversion front-end has a small form factor and uses minimal analog electronics to convert the RF signal directly to baseband (BB) or vice-versa without using any intermediate frequencies (IF). However, a low cost direct-conversion front-end can be very sensitive to any component imperfections, mainly due to manufacturing non-uniformity, leading to RF impairments such as in-phase/quadrature-phase (IQ) imbalance, carrier frequency offset (CFO), phase noise, etc. As next generation wireless systems will require even more simplified, low cost, flexible and reconfigurable front-ends, the effect of these impairments will become even more severe. Furthermore, the demand for higher carrier frequencies and constellation sizes in these wireless systems

* Corresponding author.
E-mail addresses: deepaknath.tandur@esat.kuleuven.be (D. Tandur), marc.moonen@esat.kuleuven.be (M. Moonen).
♣ EURASIP members.

0165-1684/$ - see front matter © 2010 Elsevier B.V. All rights reserved.
doi:10.1016/j.sigpro.2010.04.023

also results in a higher sensitivity to the RF impairments. The resulting distortion may lead to a dramatic performance degradation and limit the achievable data rate and so it has to be properly compensated.

The effects of RF impairments have been studied and compensation schemes for single-input single-output (SISO) based OFDM systems have been developed in [4–13]. In [6–11] efficient digital compensation schemes have been developed for the case of receiver IQ imbalance and CFO. In [10], a specially induced phase rotated short training sequence has been proposed to estimate frequency selective receiver IQ imbalance along with CFO. However, this scheme is not directly applicable in the presence of transmitter IQ imbalance in the system. Tandur and Moonen [12] and Tandur et al. [13] extend these schemes to also consider transmitter IQ imbalance along with receiver IQ imbalance and CFO.

The influence and compensation of IQ imbalance in MIMO OFDM systems have been studied in [14–17]. In [14], the authors propose a compensation scheme for receiver IQ imbalance, while in [15] and [16] a compensation scheme for combined transmitter/receiver IQ imbalance is developed. It should be noted that most papers focusing on IQ imbalance consider only frequency independent IQ imbalance. However, for wide band systems it is also essential to consider the influence of frequency selective IQ imbalance mainly arising from the mismatch of the branch components. In [17], we have considered the combined effect of frequency selective transmitter/receiver IQ imbalance, CFO and frequency selective channel distortion in a standard MIMO OFDM system.

This paper extends the work in [17] and provides a more comprehensive treatment for the compensation of CFO and IQ imbalance distortions in MIMO OFDM receivers. We *first* propose a frequency domain per tone equalizer (PTEQ) based scheme for the joint compensation of IQ imbalance and CFO along with channel distortion. This PTEQ scheme provides a unified solution for different combinations of RF impairments. *Secondly*, in the case where there is no transmitter IQ imbalance, we propose a de-coupled two stage compensation scheme. In the first stage, receiver IQ imbalance is compensated at every receiver branch along with CFO distortions. The second stage then utilizes a standard MIMO equalizer that compensates for channel distortion. We show that this two-stage approach results in lower computational complexity than a typical frequency domain joint equalization approach. The various compensation schemes are demonstrated to provide a performance close to the ideal case without RF impairments. In our simulations, we have considered a training structure similar to the MIMO extension of the uncoded IEEE 802.11a standard [18], where a short training sequence is followed by a long training sequence for the initialization of the equalizer.

The paper is organized as follows: An input–output system model for MIMO OFDM systems is developed in Section 2. Section 3 explains the joint and the de-coupled compensation schemes. Section 4 compares the complexity of the two proposed schemes in different RF impairment scenarios. The results of the numerical performance evaluation are presented in Section 5 and finally conclusions are given in Section 6.

Notation: Vectors and matrices are indicated in bold and scalar parameters in normal font. Superscripts $\{\}^*$, $\{\}^T$, $\{\}^H$, $\{\}!$ represent the complex conjugate, transpose, Hermitian and factorial function, respectively. $\mathbf{F}$ and $\mathbf{F}^{-1}$ represent the $N\times N$ discrete Fourier transform (DFT) and its inverse. $\mathbf{I}_N$ is the $N\times N$ identity matrix and $\mathbf{0}_{M\times N}$ is the $M\times N$ all-zero matrix. Operators $\otimes$, $\star$ and $\cdot$ denote the Kronecker product, convolution and component-wise vector multiplication, respectively.

2. System model

We consider a point-to-point MIMO OFDM system. Let N_t and N_r denote the number of transmit and receive antennas. We will generally assume that $N_r \geq N_t$. Then $\mathbf{S}_{(K)}$ (for $K=1\ldots N_t$) is the frequency domain OFDM symbol of size $(N\times 1)$, to be transmitted over the K th transmit antenna, where N is the number of tones. The frequency domain symbol is transformed to the time domain by the inverse discrete Fourier transform (IDFT). A cyclic prefix (CP) of length ν is then added, resulting in a time domain baseband symbol $\mathbf{s}_{(K)}$ given as

$$\mathbf{s}_{(K)} = \mathbf{P}\mathbf{F}^{-1}\mathbf{S}_{(K)} \tag{1}$$

where $\mathbf{P}$ is the cyclic prefix insertion matrix given by

$$\mathbf{P} = \left[\begin{array}{c|c} 0_{(\nu\times N-\nu)} & \mathbf{I}_\nu \\ \hline & \mathbf{I}_N \end{array}\right]$$

The time domain symbol $\mathbf{s}_{(K)}$ is parallel to serial converted and then fed to the transmitter front-end. We consider a single local oscillator (LO) supporting all the transmit (receive) antennas at the transmitter (receiver) front-end. As the LO produces only a single carrier frequency, the IQ imbalance induced by the LO is generally considered to be frequency independent (FI), i.e. it is constant over the entire OFDM symbol [5]. Due to the design restrictions, the trace lengths between the LO and the individual antenna branches may not be exactly equal and this may result in a different FI IQ imbalance for each transmit antenna. We model the transmit FI IQ imbalance as an amplitude and phase mismatch of $g_{t(K)}$ and $\phi_{t(K)}$ at the K th transmit antenna.

The other analog components in the front-end such as the digital-to-analog converters (DAC), amplifiers, low pass filters (LPFs) and mixers generally result in an overall frequency selective (FS) IQ imbalance. We represent the FS transmit IQ imbalance by two mismatched filters with frequency responses given as $\mathbf{H}_{ti(K)}=\mathbf{F}\mathbf{h}_{ti(K)}$ and $\mathbf{H}_{tq(K)}=\mathbf{F}\mathbf{h}_{tq(K)}$ at the in-phase and quadrature-phase branch of the K th transmit antenna. Here $\mathbf{h}_{ti(K)}$ and $\mathbf{h}_{tq(K)}$ represent the impulse response of the mismatched filters.

Following the derivation in [5], the equivalent baseband symbol $\mathbf{p}_{(K)}$ at the K th transmit antenna can be given as

$$\mathbf{p}_{(K)} = \mathbf{g}_{ta(K)}\star\mathbf{s}_{(K)} + \mathbf{g}_{tb(K)}\star\mathbf{s}^*_{(K)} \tag{2}$$

where

$$\mathbf{g}_{ta(K)} = \mathbf{F}^{-1}\mathbf{G}_{ta(K)} = \mathbf{F}^{-1}\left\{\frac{[\mathbf{H}_{ti(K)} + g_{t(K)}e^{-j\phi_{t(K)}}\mathbf{H}_{tq(K)}]}{2}\right\}$$

$$\mathbf{g}_{tb(K)} = \mathbf{F}^{-1}\mathbf{G}_{tb(K)} = \mathbf{F}^{-1}\left\{\frac{[\mathbf{H}_{ti(K)} - g_{t(K)}e^{j\phi_{t(K)}}\mathbf{H}_{tq(K)}]}{2}\right\} \quad (3)$$

Here $\mathbf{g}_{ta(K)}$ and $\mathbf{g}_{tb(K)}$ are mostly truncated to length L_t (and then possibly padded with $N-L_t$ zero elements). They represent the combined FI and FS IQ imbalance for the K th transmit antenna.

An expression similar to Eq. (2) can be used to model IQ imbalance at the receiver. Let $\mathbf{z}_{(J)}$ represent the down-converted baseband symbol for the J th receive antenna. This symbol is distorted by combined FS and FI IQ receiver imbalance modeled by filters $\mathbf{g}_{ra(J)}$ and $\mathbf{g}_{rb(J)}$ of length L_r, where $\mathbf{g}_{ra(J)}$ and $\mathbf{g}_{rb(J)}$ are defined similar to $\mathbf{g}_{ta(K)}$ and $\mathbf{g}_{tb(K)}$ in Eq. (2). The received symbol $\mathbf{z}_{(J)}$ can then be written as

$$\mathbf{z}_{(J)} = \mathbf{g}_{ra(J)} \star \sum_{K=1}^{N_t}(\mathbf{h}_{(J,K)} \star \mathbf{p}_{(K)}) + \mathbf{g}_{rb(J)} \star \sum_{K=1}^{N_t}(\mathbf{h}^*_{(J,K)} \star \mathbf{p}^*_{(K)}) + \underbrace{\mathbf{g}_{ra(J)} \star \mathbf{n}_{(J)} + \mathbf{g}_{rb(J)} \star \mathbf{n}^*_{(J)}}_{\mathbf{n}_{c(J)}} \quad (4)$$

where $\mathbf{h}_{(J,K)}$ is the baseband equivalent of the multipath frequency selective quasi-static channel of length L between the K th transmit and J th receive antenna. The channel is considered to be static for the duration of one entire packet consisting of training symbols and data symbols. Here $\mathbf{n}_{c(J)}$ is an improper complex noise vector derived from a zero mean additive white Gaussian noise (AWGN) vector $\mathbf{n}_{(J)}$ [20]. It can be observed that the received noise has also been modified by the IQ imbalance at the J th receive antenna. Substituting Eq. (2) in (4) leads to

$$\mathbf{z}_{(J)} = \sum_{K=1}^{N_t}[\underbrace{(\mathbf{g}_{ra(J)} \star \mathbf{h}_{(J,K)} \star \mathbf{g}_{ta(K)} + \mathbf{g}_{rb(J)} \star \mathbf{h}^*_{(J,K)} \star \mathbf{g}^*_{tb(K)})}_{\mathbf{d}_{a(J,K)}} \star \mathbf{s}_{(K)} + \underbrace{(\mathbf{g}_{ra(J)} \star \mathbf{h}_{(J,K)} \star \mathbf{g}_{tb(K)} + \mathbf{g}_{rb(J)} \star \mathbf{h}^*_{(J,K)} \star \mathbf{g}^*_{ta(K)})}_{\mathbf{d}_{b(J,K)}} \star \mathbf{s}^*_{(K)}] + \mathbf{n}_{c(J)} \quad (5)$$

where $\mathbf{d}_{a(J,K)}$, $\mathbf{d}_{b(J,K)}$ are the combined transmit IQ, channel and receive IQ impulse responses for the K th transmit and J th receive antenna. Both $\mathbf{d}_{a(J,K)}$ and $\mathbf{d}_{b(J,K)}$ are of length L_t+L+L_r-2 and are assumed to be shorter than the CP length, i.e. $(L_t+L+L_r-2 \le v)$, thus no inter-symbol-interference (ISI) between adjacent OFDM symbols.

The received symbol $\mathbf{z}_{(J)}$ is serial to parallel converted and the part corresponding to the CP is removed. The received symbol is then transformed to the frequency domain by the DFT. The frequency domain received symbol can be written as

$$\begin{aligned}\mathbf{Z}_{(J)} &= \sum_{K=1}^{N_t}[\mathbf{D}_{a(J,K)} \cdot \mathbf{S}_{(K)} + \mathbf{D}_{b(J,K)} \cdot \mathbf{S}^*_{m(K)}] + \mathbf{G}_{ra(J)} \cdot \mathbf{N}_{(J)} + \mathbf{G}_{rb(J)} \cdot \mathbf{N}^*_{m(J)} \\ &= \sum_{K=1}^{N_t}[(\mathbf{G}_{ra(J)} \cdot \mathbf{H}_{(J,K)} \cdot \mathbf{G}_{ta(K)} + \mathbf{G}_{rb(J)} \cdot \mathbf{H}^*_{m(J,K)} \cdot \mathbf{G}^*_{tb_m(K)}) \cdot \mathbf{S}_{(K)} \\ &\quad + (\mathbf{G}_{ra(J)} \cdot \mathbf{H}_{(J,K)} \cdot \mathbf{G}_{tb(K)} + \mathbf{G}_{rb(J)} \cdot \mathbf{H}^*_{m(J,K)} \cdot \mathbf{G}^*_{ta_m(K)}) \cdot \mathbf{S}^*_{m(K)}] + \mathbf{N}_{c(J)}\end{aligned} \quad (6)$$

where $\mathbf{Z}_{(J)}$, $\mathbf{D}_{a(J,K)}$, $\mathbf{D}_{b(J,K)}$, $\mathbf{H}_{(J,K)}$, $\mathbf{N}_{(J)}$ and $\mathbf{N}_{c(J)}$ are frequency domain representations of $\mathbf{z}_{(J)}$, $\mathbf{d}_{a(J,K)}$, $\mathbf{d}_{b(J,K)}$, $\mathbf{h}_{(J,K)}$, $\mathbf{n}_{(J)}$ and $\mathbf{n}_{c(J)}$. Here $(\,)_m$ denotes the mirroring operation in which the vector indices are reversed, such that $\mathbf{S}_m[l]=\mathbf{S}[l_m]$ where $l_m=2+N-l$ for $l=2\ldots N$ and $l_m=l$ for $l=1$. Note that if there is no IQ imbalance, then $\mathbf{G}_{tb(K)}=\mathbf{G}_{rb(J)}=0$ and $\mathbf{G}_{ta(K)}[l]$, $\mathbf{G}_{ra(J)}[l]$ can be considered as part of the channel, thus there is no interference from the mirror symbol $\mathbf{S}^*_{m(K)}$.

We will also consider the presence of carrier frequency offset (CFO) between the transmitter/receiver LOs. The CFO results in an additional (time domain) phase rotation proportional with time on the received symbol, which in the frequency domain results in a power leakage from every tone into every other tone [19]. We assume a CFO Δf present in the system together with transmitter/receiver IQ imbalance. The received symbol $\mathbf{z}_{(J)}$ can then be written as

$$\mathbf{z}_{(J)} = \mathbf{g}_{ra(J)} \star (\mathbf{u}_{(J)} \cdot e^{j2\pi\Delta f \cdot \mathbf{t}}) + \mathbf{g}_{rb(J)} \star (\mathbf{u}^*_{(J)} \cdot e^{-j2\pi\Delta f \cdot \mathbf{t}}) \quad (7)$$

where $\mathbf{u}_{(J)} = \sum_{K=1}^{N_t}\mathbf{h}_{(J,K)} \star \mathbf{p}_{(K)} + \mathbf{n}_{(J)}$, $e^{j\mathbf{x}}$ is the element-wise exponential function of the vector $\mathbf{x}$ and $\mathbf{t}$ is a time vector. The joint effect of transmitter/receiver IQ imbalance along with CFO and channel distortion results in a severe inter-carrier-interference (ICI) and performance degradation, as

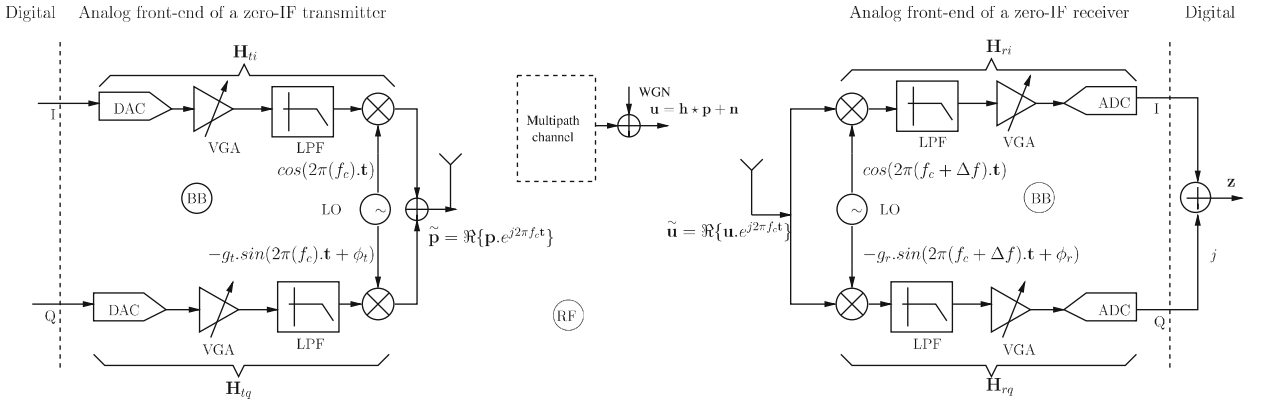


Fig. 1. Front-end direct conversion model of SISO OFDM system impaired with IQ imbalance, CFO and channel distortion.

will be shown in Section 5, and so a digital compensation scheme is needed.

Fig. 1 illustrates an end-to-end system model based on Eq. (7) for SISO OFDM with direct conversion transmitter/receiver front-ends. The figure shows the transmitter and receiver analog front-ends impaired with IQ imbalance parameters (g_t,g_r,ϕ_t,ϕ_r,$\mathbf{H}_{ti}$,$\mathbf{H}_{tq}$,$\mathbf{H}_{ri}$,$\mathbf{H}_{rq}$) and CFO (Δf). The system model also considers multipath channel distortion ($\mathbf{h}$) and the Gaussian noise ($\mathbf{n}$). A point-to-point MIMO front-end system based on the same model is also straightforwardly realizable. In the following sections, we develop generally applicable compensation schemes based on Eqs. (6) and (7).

3. IQ imbalance and CFO compensation schemes

In the presence of transmitter/receiver IQ imbalance and CFO, it is not possible to separately compensate for the transmitter/receiver IQ imbalance and for the CFO. This is because the CFO occurs after the transmit IQ imbalance and before the receive IQ imbalance introduced in the received symbol. Thus our goal is to derive a transmitter/receiver IQ imbalance compensation scheme that incorporates CFO compensation.

In order to design the compensation schemes, we first derive a strategy to estimate CFO based on some of the existing CFO estimation algorithms available in literature. We consider modified forms of two specific CFO estimation algorithms, presented in [7,10], which have opposite characteristics, i.e. the CFO estimation algorithms in [7,10] provide robust estimates in the presence of a small and large CFOs, respectively.

We consider short training symbols (STS) sequences consisting of identical symbols with no CP or guard interval inserted between them [18]. In the case of a small CFO, the estimation is based on the auto-correlation between pairs of STS available in a training sequence [7]. Let M_s identical STS of size ($N_s \times 1$) be transmitted from each of K th transmit antennas. Then $\mathbf{z}_{(J)}^{(i_s)}$ represents the baseband STS symbol as defined in Eq. (7) and i_s denotes the training symbol number in the STS sequence. The CFO estimate $\Delta\tilde{f}$ is then given as

$$\Delta\tilde{f} = \Xi\Delta\tilde{f}_{(J)} = \Xi\left(\frac{\arg\{\sum \mathbf{z}_{(J)}^{(i_s)} \cdot \mathbf{z}_{(J)}^{*(j_s)}\}}{2\pi(j_s - i_s)N_s T}\right) \tag{8}$$

where $i_s = 2 \ldots M_s - 1$, $j_s = i_s + 1 \ldots M_s$ and $j_s > i_s$ and Ξ is the expectation operator. Here T is the sampling period. Thus the total number of pairs that are considered for the calculation of the CFO is given as $N_{cfo} = C_2^{M_s-1} = (M_s-1)!/2!(M_s-4)!$.

In the case of a large CFO, the estimation is based on an non-linear least squares (NLS) algorithm [10]. Here also we consider M_s identical STS rather than the specific phase rotated STS as proposed in [10]. The choice of identical STS keeps the training requirement simple and uniform for both cases (large and small CFO). For both algorithms, a CFO $\Delta\tilde{f}_{(J)}$ is initially estimated at each individual receive antenna and then the mean of all the obtained estimates provides an overall improved CFO estimate $\Delta\tilde{f}$ for the entire system. For the time being we assume that the observed CFO estimate is sufficiently accurate, i.e. $\Delta\tilde{f} \simeq \Delta f$. Later on, we will derive an iterative scheme to correct for any residual CFO. The performance of the modified CFO estimation algorithms in the presence of IQ imbalance is further analyzed in the simulations in Section 5.

Based on the observed CFO estimate, we first develop an efficient joint compensation scheme in Section 3.1. In Section 3.2, we derive a de-coupled compensation scheme for the case where there is no transmit IQ imbalance, and where the estimation and compensation of receiver IQ imbalance is performed independently of the channel distortion.

3.1. Joint transmitter/receiver IQ imbalance and CFO compensation schemes

Once the CFO is known (with $\Delta\tilde{f} \simeq \Delta f$), we can use a cascade of a time domain equalizer (TEQ) and a frequency domain equalizer (FEQ). The compensation is then performed in the reverse order of their appearance, i.e. starting with the receiver IQ imbalance and CFO compensation in the time domain, and then a joint compensation of the channel distortion and the transmitter IQ imbalance in the frequency domain. Later we merge the entire equalization structure to form one unified per tone equalizer (PTEQ) in the frequency domain.

We design TEQ with two filter branches $\mathbf{v}_{a(J)}$ and $\mathbf{v}_{b(J)}$ for every receive antenna ($J = 1 \ldots N_r$). Both $\mathbf{v}_{a(J)}$ and $\mathbf{v}_{b(J)}$ have L_r taps. The filter $\mathbf{v}_{a(J)}$ is applied to the symbol $\mathbf{z}_{(J)}$ and the filter $\mathbf{v}_{b(J)}$ is applied to $\mathbf{z}_{(J)}^*$. This leads to

$$\begin{aligned}\mathbf{z}_{q(J)} &= \mathbf{v}_{a(J)} \star \mathbf{z}_{(J)} + \mathbf{v}_{b(J)} \star \mathbf{z}_{(J)}^* \\ &= \underbrace{(\mathbf{v}_{a(J)} \star \mathbf{g}_{ra(J)} + \mathbf{v}_{b(J)} \star \mathbf{g}_{rb(J)}^*)}_{\mathbf{f}_{1(J)}} \star (\mathbf{u}_{(J)} \cdot e^{\mathrm{j}2\pi\Delta f \cdot \mathbf{t}}) \\ &\quad + \underbrace{(\mathbf{v}_{a(J)} \star \mathbf{g}_{rb(J)} + \mathbf{v}_{b(J)} \star \mathbf{g}_{ra(J)}^*)}_{\mathbf{f}_{2(J)}} \star (\mathbf{u}_{(J)}^* \cdot e^{-\mathrm{j}2\pi\Delta f \cdot \mathbf{t}})\end{aligned} \tag{9}$$

The design target for the TEQ filters $\mathbf{v}_{a(J)}$ and $\mathbf{v}_{b(J)}$ is such that the term $\mathbf{f}_{2(J)}$ vanishes in Eq. (9). The solutions to this set of equations are $\mathbf{v}_{a(J)} = \mathbf{g}_{ra(J)}^* \alpha$ and $\mathbf{v}_{b(J)} = -\mathbf{g}_{rb(J)} \alpha$ where α is a non-zero scalar. Thus with appropriate coefficient values for $\mathbf{v}_{a(J)}$ and $\mathbf{v}_{b(J)}$, we can have $\mathbf{z}_{q(J)}$ free of any contributions from $\mathbf{u}_{(J)}^*$, i.e. free from receiver IQ imbalance.

Once the receiver IQ imbalance has been compensated by the TEQ, we can de-rotate $\mathbf{z}_{q(J)}$ with $e^{-\mathrm{j}2\pi\Delta\tilde{f}\cdot\mathbf{t}}$. This leads to

$$\tilde{\mathbf{z}}_{q(J)} = \mathbf{z}_{q(J)} \cdot e^{-\mathrm{j}2\pi\Delta\tilde{f}\cdot\mathbf{t}} = \tilde{\mathbf{f}}_{1(J)} \star \mathbf{u}_{(J)} \tag{10}$$

where $\tilde{\mathbf{f}}_{1(J)} = \mathbf{f}_{1(J)} \cdot (e^{-\mathrm{j}2\pi\Delta\tilde{f}\cdot(0\ldots(L_r-1))^T})$ is a modulated version of $\mathbf{f}_{1(J)}$. The resulting vector $\tilde{\mathbf{z}}_{q(J)}$ is free from CFO and contains only transmitter IQ imbalance along with channel distortion. The resulting filter $\tilde{\mathbf{f}}_{1(J)}$ may be considered to be part of the overall channel filtering. Each filtered sequence $\tilde{\mathbf{z}}_{q(J)}$ (stacked into an N vector) can be transformed into a frequency domain vector $\tilde{\mathbf{Z}}_{q(J)}$ and then a FEQ is applied, to compensate for the remaining distortions and obtain an estimate of the transmitted

symbol, given as

$$\begin{bmatrix} \widetilde{\mathbf{S}}_{(1)}[l] \\ \vdots \\ \widetilde{\mathbf{S}}_{(N_t)}[l] \end{bmatrix} = \begin{bmatrix} \mathbf{W}_{a(1,1)}[l] & \mathbf{W}_{b(1,1)}[l] & \cdots & \mathbf{W}_{a(N_r,1)}[l] & \mathbf{W}_{b(N_r,1)}[l] \\ \vdots & \vdots & & \vdots & \\ \mathbf{W}_{a(1,N_t)}[l] & \mathbf{W}_{b(1,N_t)}[l] & \cdots & \mathbf{W}_{a(N_r,N_t)}[l] & \mathbf{W}_{b(N_r,N_t)}[l] \end{bmatrix} \begin{bmatrix} \widetilde{\mathbf{Z}}_{q(1)}[l] \\ \widetilde{\mathbf{Z}}^{*}_{q(1)}[l_m] \\ \vdots \\ \widetilde{\mathbf{Z}}_{q(N_r)}[l] \\ \widetilde{\mathbf{Z}}^{*}_{q(N_r)}[l_m] \end{bmatrix} \tag{11}$$

where $\mathbf{W}_{a(J,K)}[l]$ and $\mathbf{W}_{b(J,K)}[l]$ are the coefficients of the FEQ.

In order to simplify the entire compensation scheme, we transform the TEQ into the frequency domain and then merge the resultant structure with the FEQ. The equalization is then performed for each tone separately with an L_r tap per tone equalizer (PTEQ). We refer to [21] for a detailed description of the PTEQ and its advantages.

To transform the TEQ+FEQ scheme into a PTEQ scheme, we first swap the TEQ filtering operation (Eq. (9)) with the de-rotation with $e^{-\mathrm{j}2\pi\Delta\tilde{f}\cdot\mathbf{t}}$ (Eq. (10)). This results in a modified form (with modified equalizer coefficients $\mathbf{v}_{a(J)}$ and $\mathbf{v}_{b(J)}$) of Eq. (10) given as

$$\begin{aligned} \tilde{\mathbf{z}}_{q(J)} &= \mathbf{v}_{a(J)} \star (\mathbf{z}_{(J)} \cdot e^{-\mathrm{j}2\pi\Delta\tilde{f}\cdot\mathbf{t}}) + \mathbf{v}_{b(J)} \star (\mathbf{z}^{*}_{(J)} \cdot e^{-\mathrm{j}2\pi\Delta\tilde{f}\cdot\mathbf{t}}) \\ &= \underbrace{(\mathbf{v}_{a(J)} \star \tilde{\mathbf{g}}_{ra(J)} + \mathbf{v}_{b(J)} \star \tilde{\mathbf{g}}^{*}_{rb(J)})}_{\mathbf{f}_{1(J)}} \star \mathbf{u}_{(J)} \\ &\quad + \underbrace{(\mathbf{v}_{a(J)} \star \tilde{\mathbf{g}}_{rb(J)} + \mathbf{v}_{b(J)} \star \tilde{\mathbf{g}}^{*}_{ra(J)})}_{\mathbf{f}_{2(J)}} \star (\mathbf{u}^{*}_{(J)} \cdot e^{-2\mathrm{j}2\pi\Delta\tilde{f}\cdot\mathbf{t}}) \end{aligned} \tag{12}$$

Here $\tilde{\mathbf{g}}_{ra(J)} = \mathbf{g}_{ra(J)} \cdot (e^{-\mathrm{j}\tilde{\mathbf{w}}})$, $\tilde{\mathbf{g}}_{rb(J)} = \mathbf{g}_{rb(J)} \cdot (e^{\mathrm{j}\tilde{\mathbf{w}}})$ with $\tilde{\mathbf{w}} = 2\pi\Delta\tilde{f} \cdot (0 \ldots (L_r - 1))^{T}$. To suppress $\mathbf{u}^{*}_{(J)}$ in Eq. (12), we now require $\mathbf{v}_{a(J)} = \tilde{\mathbf{g}}^{*}_{ra(J)}\alpha$ and $\mathbf{v}_{b(J)} = -\tilde{\mathbf{g}}_{rb(J)}\alpha$. The swapping of the de-rotation with the TEQ filtering effectively results in a modulated version of the original TEQ filters (so still linear filters but with adjusted filter coefficients). The TEQ filtering is then transformed to the frequency domain resulting in a PTEQ employing two DFT operations and $L_p = L_r - 1$ difference terms [21]. Eq. (12) can then be written as

$$\tilde{\mathbf{Z}}_{q(J)}[l] = \begin{bmatrix} \mathbf{V}_{a(J)}[l] \\ \mathbf{V}_{b(J)}[l] \end{bmatrix}^{T} \begin{bmatrix} \mathbf{F}_{ext}[l]\mathbf{z}_{(J)} \cdot e^{-\mathrm{j}2\pi\Delta\tilde{f}\cdot\mathbf{t}} \\ \mathbf{F}_{ext}[l]\mathbf{z}^{*}_{(J)} \cdot e^{-\mathrm{j}2\pi\Delta\tilde{f}\cdot\mathbf{t}} \end{bmatrix} \tag{13}$$

where $\mathbf{V}_{a(J)}[l]$ and $\mathbf{V}_{b(J)}[l]$ are PTEQ filter vectors of size $(L_r \times 1)$. Here $\mathbf{F}_{ext}[l]$ is defined as

$$\mathbf{F}_{ext}[l] = \begin{bmatrix} \mathbf{I}_{L_r-1} & 0_{L_r-1\times N-L_r+1} & -\mathbf{I}_{L_r-1} \\ 0_{1\times L_r-1} & \mathbf{F}[l] & \end{bmatrix}$$

The first block row in $\mathbf{F}_{ext}[l]$ is seen to extract the difference terms, while the last row corresponds to a DFT, where $\mathbf{F}[l]$ is the $[l]$th row of the DFT matrix. The PTEQ filter coefficients $\mathbf{V}_{k(J)}[l]$ (for $k = a,b$) are related to the TEQ coefficients as follows:

$$\begin{bmatrix} \mathbf{V}_{k_0(J)}[l] \\ \mathbf{V}_{k_1(J)}[l] \\ \vdots \\ \mathbf{V}_{k_{L_r-1}(J)}[l] \end{bmatrix} = \begin{bmatrix} (\beta_l)^0 & (\beta_l)^1 & \ldots & (\beta_l)^{L_r-1} \\ 0 & (\beta_l)^0 & \ldots & (\beta_l)^{L_r-2} \\ \vdots & \vdots & \ddots & \vdots \\ 0 & 0 & \ldots & (\beta_l)^0 \end{bmatrix} \begin{bmatrix} \mathbf{v}_{k_0(J)} \\ \mathbf{v}_{k_1(J)} \\ \vdots \\ \mathbf{v}_{k_{L_r-1}(J)} \end{bmatrix}$$

where $\beta_l = e^{-\mathrm{j}2\pi((l-1)/N)}$ and the subscript x in $\mathbf{V}_{k_x(J)}[l]$ and $\mathbf{v}_{k_x(J)}$ represents the filter tap index. We can now compensate for the remaining distortions by applying a $2(N_t \times N_r)$ FEQ to the received symbol $\tilde{\mathbf{Z}}_{q(J)}[l]$ and $\tilde{\mathbf{Z}}^{*}_{q(J)}[l_m]$ as in Eq. (11).

As a final step, we merge the PTEQ (13) and the FEQ (11) into a four branch PTEQ. The transmitted symbol estimate is then obtained as

$$\begin{aligned} \tilde{\mathbf{S}}_{(K)}[l] &= \sum_{J=1}^{N_r} \left(\mathbf{W}_{a(J,K)}[l] \begin{bmatrix} \mathbf{V}_{a(J)}[l] \\ \mathbf{V}_{b(J)}[l] \end{bmatrix}^{T} \begin{bmatrix} \mathbf{F}_{ext}[l]\mathbf{z}_{(J)} \cdot e^{-\mathrm{j}2\pi\Delta\tilde{f}\cdot\mathbf{t}} \\ \mathbf{F}_{ext}[l]\mathbf{z}^{*}_{(J)} \cdot e^{-\mathrm{j}2\pi\Delta\tilde{f}\cdot\mathbf{t}} \end{bmatrix} \right. \\ &\quad \left. + \mathbf{W}_{b(J,K)}[l] \begin{bmatrix} \mathbf{V}^{*}_{a(J)}[l_m] \\ \mathbf{V}^{*}_{b(J)}[l_m] \end{bmatrix}^{T} \begin{bmatrix} (\mathbf{F}_{ext}[l_m]\mathbf{z}_{(J)} \cdot e^{-\mathrm{j}2\pi\Delta\tilde{f}\cdot\mathbf{t}})^{*} \\ (\mathbf{F}_{ext}[l_m]\mathbf{z}^{*}_{(J)} \cdot e^{-\mathrm{j}2\pi\Delta\tilde{f}\cdot\mathbf{t}})^{*} \end{bmatrix} \right) \\ &= \sum_{J=1}^{N_r} \underbrace{\begin{bmatrix} \mathbf{V}_{a(J,K)}[l] \\ \mathbf{V}_{b(J,K)}[l] \\ \mathbf{V}_{c(J,K)}[l] \\ \mathbf{V}_{d(J,K)}[l] \end{bmatrix}^{T}}_{\mathbf{V}^{T}_{ext(J,K)}[l]} \underbrace{\begin{bmatrix} \mathbf{F}_{ext}[l]\mathbf{z}_{(J)} \cdot e^{-\mathrm{j}2\pi\Delta\tilde{f}\cdot\mathbf{t}} \\ \mathbf{F}_{ext}[l]\mathbf{z}^{*}_{(J)} \cdot e^{-\mathrm{j}2\pi\Delta\tilde{f}\cdot\mathbf{t}} \\ (\mathbf{F}_{ext}[l_m]\mathbf{z}_{(J)} \cdot e^{-\mathrm{j}2\pi\Delta\tilde{f}\cdot\mathbf{t}})^{*} \\ (\mathbf{F}_{ext}[l_m]\mathbf{z}^{*}_{(J)} \cdot e^{-\mathrm{j}2\pi\Delta\tilde{f}\cdot\mathbf{t}})^{*} \end{bmatrix}}_{\mathbf{z}_{ext(J)}[l]} \end{aligned} \tag{14}$$

where $\mathbf{V}_{a(J,K)}[l] = (\mathbf{W}_{a(J,K)}[l]\mathbf{V}_{a(J)}[l])$, $\mathbf{V}_{b(J,K)}[l] = (\mathbf{W}_{a(J,K)}[l]\mathbf{V}_{b(J)}[l])$, $\mathbf{V}_{c(J,K)}[l] = (\mathbf{W}_{b(J,K)}[l]\mathbf{V}^{*}_{a(J)}[l_m])$ and $\mathbf{V}_{d(J,K)}[l] = (\mathbf{W}_{b(J,K)}[l]\mathbf{V}^{*}_{b(J)}[l_m])$ are filter vectors of size $(L_r \times 1)$.

The estimate of PTEQ coefficients $\tilde{\mathbf{V}}_{ext(J,K)}[l]$ can now be obtained from a sequence of M_l so-called long training symbols (LTS) that are also constructed based on Eq. (1). The PTEQ coefficients can then be obtained as follows:

$$\begin{aligned} &\begin{bmatrix} \tilde{\mathbf{V}}_{ext(1,1)}[l] & \ldots & \tilde{\mathbf{V}}_{ext(1,N_t)}[l] \\ \vdots & \vdots & \vdots \\ \tilde{\mathbf{V}}_{ext(N_r,1)}[l] & \ldots & \tilde{\mathbf{V}}_{ext(N_r,N_t)}[l] \end{bmatrix} \\ &= \underbrace{\begin{bmatrix} \mathbf{Z}^{(1)}_{ext(1)}[l] & \ldots & \mathbf{Z}^{(1)}_{ext(N_r)}[l] \\ \vdots & \vdots & \vdots \\ \mathbf{Z}^{(M_l)}_{ext(1)}[l] & \ldots & \mathbf{Z}^{(M_l)}_{ext(N_r)}[l] \end{bmatrix}^{\dagger}}_{\mathbf{Z}_{ext_tot-[l]}} \begin{bmatrix} \mathbf{S}^{(1)}_{(1)}[l] & \ldots & \mathbf{S}^{(1)}_{(N_t)}[l] \\ \vdots & \vdots & \vdots \\ \mathbf{S}^{(M_l)}_{(1)}[l] & \ldots & \mathbf{S}^{(M_l)}_{(N_t)}[l] \end{bmatrix} \end{aligned} \tag{15}$$

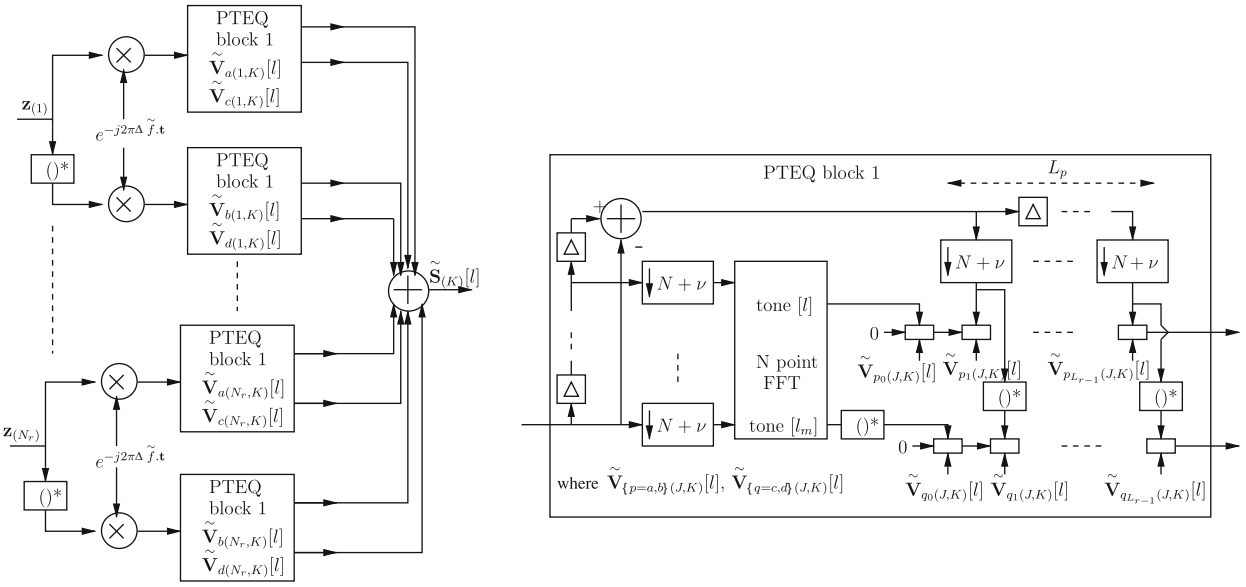


Fig. 2. Joint compensation scheme for MIMO OFDM system impaired with transmitter/receiver IQ imbalance and CFO.

where † is the pseudo-inverse operation and the superscript (i) in $\mathbf{Z}^{(i)}_{ext(J)}[l]$) and $\mathbf{S}^{(i)}_{(K)}[l]$ represents the training symbol number in the LTS sequence. The final PTEQ compensation scheme is shown in Fig. 2.

Eqs. (14) and (15) show that in order to estimate the PTEQ coefficients an LTS sequence of length $M_l \geq 4L_rNr$ is needed. A longer training sequence will provide improved estimates due to a better noise averaging. The total number of PTEQ coefficients to be estimated is $4L_r(N_t \times N_r)$ per tone. In the case where $M_l=4L_rNr$, the training symbols at tone $[l]$ and $[l_m]$ of every LTS are required to be linearly independent of each other and also independent of tone $[l]$ and $[l_m]$ of the LTS transmitted from other transmit antennas. This is required so that the pseudo-inverse operation on the matrix $\mathbf{Z}_{ext_tot}[l]$ always generates a unique solution. The transmission packet for the joint compensation scheme now consists of identical STS sequences for CFO estimation, followed by linearly independent LTS sequences for the estimation of PTEQ coefficients, and finally the data sequences. The STS and LTS sequences can be taken from any suitable alphabet. The packet structure for the joint compensation scheme before parallel to serial conversion at the front-end is shown in Fig. 3(a).

Note:

- *Residual CFO error correction*: We have derived Eq. (14) assuming that we accurately know Δf. In practice, the CFO estimation algorithm may not be precise leading to a non-zero $e_{\Delta f}=\Delta f-\Delta\tilde{f}$, and hence a residual CFO effect in $\mathbf{Z}_{ext(J)}[l]$. This then leads to a poor $\tilde{\mathbf{S}}_{(K)}[l]$ symbol estimate due to residual ICI. The performance of the PTEQ can be improved by searching amongst various PTEQs and CFO values $\Delta\tilde{f}$ such that the error in $(\mathbf{S}^{(i)}_{(K)}[l]-\tilde{\mathbf{S}}^{(i)}_{(K)}[l])$ for $i=1\ldots M_l$ is minimized. As we assume to already have a good (initial) CFO estimate, the search amongst CFOs is now restricted to a narrow range of values. In general, this indeed leads to a much more accurate estimation of the CFO (see section **5**). The PTEQ coefficients thus obtained are finally used for compensation.
- *Insufficient CP length*: It should be noted that the PTEQ scheme can also be applied in the case of insufficient CP length, i.e. when the CP is shorter than the overall combined channel length ($\nu < L_t+L+L_r+L_r-3$). In this case, besides ICI within the OFDM symbol due to IQ imbalance and CFO, there is also ISI from adjacent OFDM symbols. To compensate for the combined ICI and ISI effect, the PTEQ length may have to be increased to include a channel shortening operation and obtain sufficient improvement in performance [12]. The influence of ISI has not been considered in this paper in order to keep the data model simple.
- *Generalized structure*: The PTEQ scheme proposed here is a general structure that can be simplified for specific scenarios. These scenarios are discussed here:
  - *Only receiver IQ imbalance and CFO*: In this case, the coefficients $\mathbf{V}_{c(J,K)}[l]$ and $\mathbf{V}_{d(J,K)}[l]$ can be set to zero. As a result the PTEQ structure will now have only two active branches corresponding to coefficients $\mathbf{V}_{a(J,K)}[l]$ and $\mathbf{V}_{b(J,K)}[l]$. The equalizer structure still requires two DFT branches but now followed by a two branch PTEQ. The total number of PTEQ coefficients to be estimated is $2L_r(N_t \times N_r)$ per tone and hence the required LTS sequence length is $M_l \geq 2L_rNr$.
  - *Only transmitter/receiver IQ imbalance and no CFO*: In this case, the entire estimation and compensation

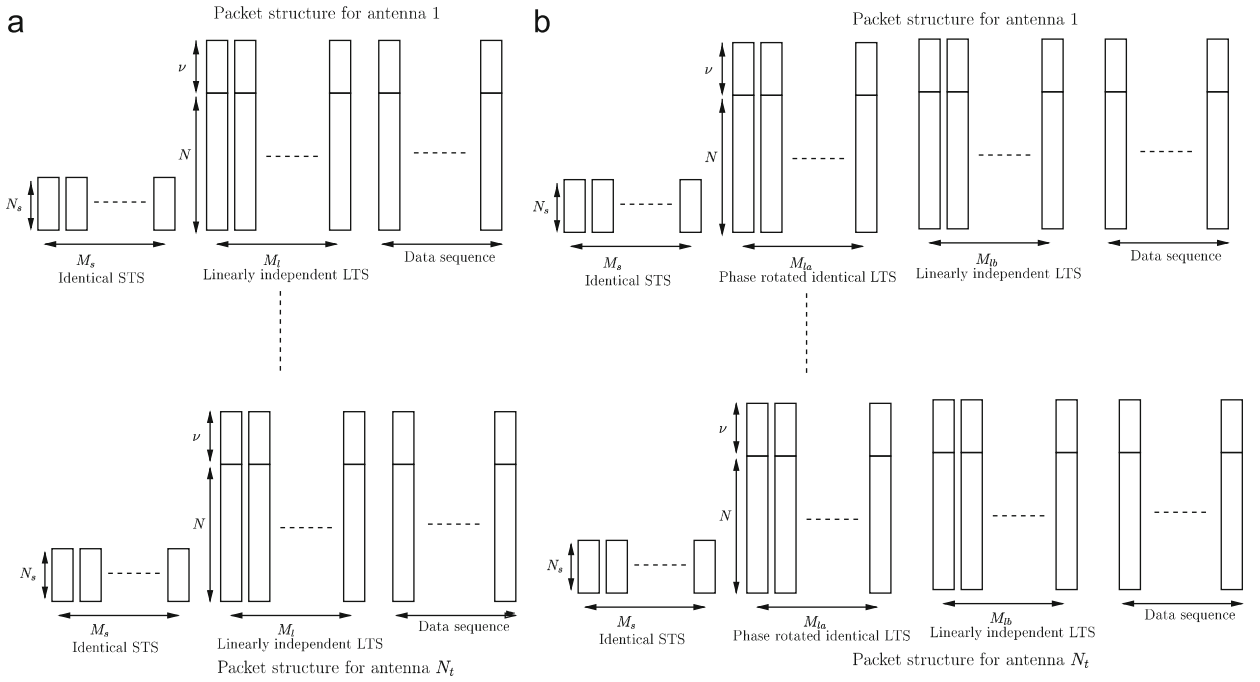


Fig. 3. Packet structure containing STS, LTS and data sequence before parallel to serial conversion at the transmitter: (a) joint compensation scheme, (b) de-coupled compensation scheme.

of transmitter/receiver IQ imbalance can straightforwardly be performed in the frequency domain by the FEQ as shown in Eq. (11). The compensation of transmitter/receiver IQ imbalance is completely based on the suppression of the interference from the mirror tone. Thus the contribution of the TEQ filters is not required in the PTEQ equalization structure. The PTEQ length can now be set to $L_r=1$. The coefficients $\mathbf{V}_{b(J,K)}[l]$ and $\mathbf{V}_{d(J,K)}[l]$ can also be set to zero, thus the PTEQ is reduced to a first order filter based on Eq. (11), similar to the joint compensation scheme in [14–16]. It should be noted that the FEQ equalization structure is also valid in the presence of either only transmitter IQ imbalance or only receiver IQ imbalance. The total number of coefficients to be estimated is $2(N_t \times N_r)$ per tone and hence the required LTS sequence length is $M_l \geq 2Nr$.

- *FI receiver IQ imbalance, FS transmitter IQ imbalance and CFO*: This corresponds to the case of no filter mismatch at the receiver front-end. In this case the impulse response of the perfectly matched receiver front-end filters is considered as part of the channel. Thus the TEQ filters $\mathbf{v}_{a(J)}$ and $\mathbf{v}_{b(J)}$ can be set to length $L_r=1$, where they now compensate only for FI receiver IQ imbalance. As a result the PTEQ length is also set to $L_r=1$. It should be noted that the length of the PTEQ is not affected by filter mismatch at the transmitter front-end, as the compensation of transmitter IQ imbalance is always performed in the frequency domain based on the suppression of interference from the mirror tone. The total number of coefficients to be estimated is $4(N_t \times N_r)$ per tone and hence the required LTS sequence length is $M_l \geq 4Nr$.

3.2. De-coupled compensation schemes for scenarios without transmitter IQ imbalance

So far we have considered digital compensation schemes for joint transmitter/receiver frequency selective IQ imbalance, CFO and channel distortion. In this section, we derive compensation schemes in the case where there is no transmitter IQ imbalance. The case of only receiver IQ imbalance and no transmitter IQ imbalance can be considered as a typical downstream communication scenario between a base station and a mobile device. The mobile device is considered to be low power, inexpensive and so may not have ideal front-end characteristics. As a result the mobile device may be impaired with receiver IQ imbalance distortions. The base station is usually considered to have an ideal front-end. We show that in the case where there is no transmitter IQ imbalance, the receiver IQ imbalance compensation can be de-coupled from the channel equalization resulting in a compensation in two stages. The first stage compensates for receiver IQ imbalance and CFO, and the second stage then compensates for remaining channel distortion. We will show that this two-stage approach results in lower computational complexity.

3.2.1. Receiver IQ imbalance and CFO compensation

The PTEQ scheme proposed in Section 3.1 provides a solution for each and every combination of impairments, but may be quite expensive in specific scenarios as it requires $4L_r(N_t \times N_r)$ equalizer taps to be estimated per tone. In this section we develop an estimation scheme for the TEQ filters, $\mathbf{v}_{a(J)}$ and $\mathbf{v}_{b(J)}$ in Eq. (9), for the case where there is receiver IQ imbalance and CFO, but no transmitter IQ imbalance. As the TEQ coefficients are dependent only on receiver IQ imbalance parameters, once trained, they remain fixed even under variations in channel characteristics. The TEQ is again transformed to the frequency domain resulting in a two branch PTEQ as shown in Eq. (13). The output of this PTEQ can then be fed to the FEQ for channel distortion compensation.

In order to remove the indeterminacy in the estimation of the two filters $\mathbf{v}_{a(J)}$ and $\mathbf{v}_{b(J)}$ (Section 3.1), we set the first tap of $\mathbf{v}_{a(J)}$ to 1, thus the coefficients of $\mathbf{v}_{a(J)}$ are given as $[1,\mathbf{v}_{a_1(J)},\ldots,\mathbf{v}_{a_{L_r-1}(J)}]$. The coefficients of $\mathbf{v}_{b(J)}$ are $[\mathbf{v}_{b_0(J)},\mathbf{v}_{b_1(J)},\ldots,\mathbf{v}_{b_{L_r-1}(J)}]$. The design target for the filters in Eq. (9) is then given as $\mathbf{v}_{a(J)}=\mathbf{g}^*_{ra(J)}/\mathbf{g}^*_{ra0(J)}$ and $\mathbf{v}_{b(J)}=-\mathbf{g}_{rb(J)}/\mathbf{g}^*_{ra0(J)}$.

We now consider a specific sequence of M_{la} so-called phase rotated LTS. All the training symbols are identical up to a different phase rotation $e^{j\Phi^{(i)}}$ where i represents the training symbol number, i.e. $\mathbf{S}^{(i)}_{(K)}=\mathbf{S}_{(K)}e^{j\Phi^{(i)}}$. The phase rotation term $\Phi^{(i)}$ can be between $0\ldots2\pi$ radians. Now Eq. (9) can be re-written for the ith training symbol as follows:

$$\mathbf{z}^{(i)}_{q(J)}=\mathbf{z}^{(i)}_{(J)}\star\mathbf{v}_{a(J)}+\mathbf{z}^{*(i)}_{(J)}\star\mathbf{v}_{b(J)}$$

$$\begin{bmatrix}\mathbf{z}^{(i)}_{q_1(J)}\\ \vdots\\ \mathbf{z}^{(i)}_{q_N(J)}\end{bmatrix}=\left[\begin{array}{ccc|c}\mathbf{z}^{(i)}_{1(J)} & \mathbf{z}^{(i)}_{\nu(J)} & \cdots & \mathbf{z}^{(i)}_{\nu-L_r+1(J)}\\ \vdots & \vdots & & \vdots\\ \mathbf{z}^{(i)}_{N(J)} & \mathbf{z}^{(i)}_{N-1(J)} & \cdots & \mathbf{z}^{(i)}_{N-L_r+1(J)}\end{array}\right]\left[\begin{array}{c}1\\ \mathbf{v}_{a_1(J)}\\ \vdots\\ \mathbf{v}_{a_{L_r-1}(J)}\end{array}\right]+\left[\begin{array}{ccc|c}\mathbf{z}^{*(i)}_{1(J)} & \mathbf{z}^{*(i)}_{\nu(J)} & \cdots & \mathbf{z}^{*(i)}_{\nu-L_r+2(J)}\\ \vdots & \vdots & & \vdots\\ \mathbf{z}^{*(i)}_{N(J)} & \mathbf{z}^{*(i)}_{N-1(J)} & \cdots & \mathbf{z}^{*(i)}_{N-L_r+1(J)}\end{array}\right]\left[\begin{array}{c}\mathbf{v}_{b_0(J)}\\ \mathbf{v}_{b_1(J)}\\ \vdots\\ \mathbf{v}_{b_{L_r-1}(J)}\end{array}\right] \tag{16}$$

where the subscript x in $\mathbf{z}^{(i)}_{q_x(J)}$ and $\mathbf{z}^{(i)}_{x(J)}$ represents the time index. We can then relate pairs of $\mathbf{z}^{(i)}_{q(J)}$ vectors as

$$\mathbf{z}^{(j)}_{q(J)}=e^{j\Omega}\mathbf{z}^{(i)}_{q(J)}$$

$$\mathbf{v}_{a(J)}\star(\underbrace{\mathbf{z}^{(j)}_{(J)}-e^{j\Omega}\mathbf{z}^{(i)}_{(J)}}_{\mathbf{x}^{(j,i)}_{(J)}})=\underbrace{(e^{j\Omega}\mathbf{z}^{*(i)}_{(J)}-\mathbf{z}^{*(j)}_{(J)})}_{\mathbf{Y}^{(j,i)}_{(J)}}\star\mathbf{v}_{b(J)} \tag{17}$$

where $\Omega=2\pi(j-i)\Delta fNT+\Phi^{(j)}-\Phi^{(i)}$, $i=1\ldots M_{la}-1$, $j=i+1\ldots M_{la}$ and $j>i$. Eq. (17) can be written in matrix form as

$$\left[\begin{array}{ccc|c}\mathbf{X}^{(2,1)}_{1(J)} & \mathbf{X}^{(2,1)}_{\nu(J)} & \cdots & \mathbf{X}^{(2,1)}_{\nu-L_r+2(J)}\\ \vdots & \vdots & & \vdots\\ \mathbf{X}^{(2,1)}_{N(J)} & \mathbf{X}^{(2,1)}_{N-1(J)} & \cdots & \mathbf{X}^{(2,1)}_{N-L_r+1(J)}\\ \mathbf{X}^{(3,1)}_{1(J)} & \mathbf{X}^{(3,1)}_{\nu(J)} & & \mathbf{X}^{(3,1)}_{\nu-L_r+2(J)}\\ \vdots & \vdots & & \vdots\\ \underbrace{\mathbf{X}^{(M_l,M_l-1)}_{N(J)}}_{\mathbf{A}_{1(J)}} & \underbrace{\mathbf{X}^{(M_l,M_l-1)}_{N-1(J)}}_{\mathbf{A}_{2(J)}} & \cdots & \mathbf{X}^{(M_l,M_l-1)}_{N-L_r+1(J)}\end{array}\right]\left[\begin{array}{c}1\\ \mathbf{v}_{a_1(J)}\\ \vdots\\ \mathbf{v}_{a_{L_r-1}(J)}\end{array}\right]=$$

$$\left[\begin{array}{ccc|c}\mathbf{Y}^{(2,1)}_{1(J)} & \mathbf{Y}^{(2,1)}_{\nu(J)} & \cdots & \mathbf{Y}^{(2,1)}_{\nu-L_r+2(J)}\\ \vdots & \vdots & & \vdots\\ \mathbf{Y}^{(2,1)}_{N(J)} & \mathbf{Y}^{(2,1)}_{N-1(J)} & \cdots & \mathbf{Y}^{(2,1)}_{N-L_r+1(J)}\\ \mathbf{Y}^{(3,1)}_{1(J)} & \mathbf{Y}^{(3,1)}_{\nu(J)} & & \mathbf{Y}^{(3,1)}_{\nu-L_r+2(J)}\\ \vdots & \vdots & & \vdots\\ \underbrace{\mathbf{Y}^{(M_l,M_l-1)}_{N(J)} & \mathbf{Y}^{(M_l,M_l-1)}_{N-1(J)}}_{\mathbf{B}_{(J)}} & \cdots & \mathbf{Y}^{(M_l,M_l-1)}_{N-L_r+1(J)}\end{array}\right]\left[\begin{array}{c}\mathbf{v}_{b_0(J)}\\ \mathbf{v}_{b_1(J)}\\ \vdots\\ \mathbf{v}_{b_{L_r-1}(J)}\end{array}\right] \tag{18}$$

Based on this the TEQ coefficients can be estimated as

$$\underbrace{[\tilde{\mathbf{v}}_{b_0(J)}|\ldots|\tilde{\mathbf{v}}_{b_{L_r-1}(J)}\tilde{\mathbf{v}}_{a_1(J)}|\ldots|\tilde{\mathbf{v}}_{a_{L_r-1}(J)}]^T}_{\tilde{\mathbf{v}}^T_{ab(J)}}=[\mathbf{B}_{(J)}|-\mathbf{A}_{2(J)}]^{\dagger}\mathbf{A}_{1(J)} \tag{19}$$

where $\tilde{\mathbf{v}}_{a_x(J)}$ and $\tilde{\mathbf{v}}_{b_x(J)}$ are estimates of $\mathbf{v}_{a_x(J)}$ and $\mathbf{v}_{b_x(J)}$, respectively. Eqs. (17)–(19) show that the total number of valid pairs (i,j) that can be considered is $N_p=C^{M_l}_2-N_\Omega$ where $C^b_a=b!/a!(b-a)!$ and N_Ω is the total number of pairs with $\Omega=0,\pi$ and 2π radians. We do not consider tone pairs with $\Omega=0,\pi,2\pi$ as these lead to ill-conditioning in the case of a zero CFO. The formula for N_p shows that as the number of training symbols is increased, additional tone pairs can be included in Eqs. (18) and (19), leading to an improved estimation. The only requirements for Eq. (19) to be valid is that the total number of compensation coefficients to be estimated $(2L_r-1)$ for every J th receive antenna should always be smaller than the OFDM symbol size N, and the phase rotated LTS sequence length $M_{la}\geq 2$.

Once the TEQ coefficients are known, the symbol $\mathbf{z}_{q(J)}$ is de-rotated by $e^{-j2\pi\Delta\tilde{f}\cdot\mathbf{t}}$ as shown in Eq. (10). The de-rotated symbol $\tilde{\mathbf{z}}_{q(J)}$ is transformed into a frequency domain vector $\tilde{\mathbf{Z}}_{q(J)}$, and then a second stage FEQ, now based on a standard MIMO channel equalizer is applied to recover the transmitted symbols

$$\begin{bmatrix}\tilde{\mathbf{S}}_{(1)}[l]\\ \vdots\\ \tilde{\mathbf{S}}_{(N_t)}[l]\end{bmatrix}=\begin{bmatrix}\mathbf{W}_{a(1,1)}[l] & \cdots & \mathbf{W}_{a(N_r,1)}[l]\\ \vdots & \vdots & \vdots\\ \mathbf{W}_{a(1,N_t)}[l] & \cdots & \mathbf{W}_{a(N_r,N_t)}[l]\end{bmatrix}\begin{bmatrix}\tilde{\mathbf{Z}}_{q(1)}[l]\\ \vdots\\ \tilde{\mathbf{Z}}_{q(N_r)}[l]\end{bmatrix} \tag{20}$$

Eq. (20) is a reduced form of Eq. (11) with only half as many FEQ coefficients to be estimated. The number of coefficients to be estimated for the FEQ is now $N_t\times N_r$ per tone and hence the required LTS sequence length is $M_{lb}\geq Nr$. As the FEQ filters are not required to compensate for any mirror image interference, the training symbols transmitted on tone $[l]$ should only be

linearly independent of training symbols transmitted from other transmit antennas on tone $[l]$. The transmission packet for the de-coupled compensation scheme consists of identical STS sequences for CFO estimation, followed by phase rotated identical LTS for receiver IQ imbalance compensation, linearly independent LTS sequences for the estimation of FEQ coefficients, and finally the data sequences. The STS and LTS sequences can be taken from any suitable alphabet. The packet structure for the de-coupled compensation scheme is shown in Fig. 3(b).

Finally, following (12) and (13), we can swap the de-rotation operation with the TEQ filters and then the TEQ filters can be transformed to the frequency domain resulting in a two stage (**2S-PTEQ/FEQ**) scheme. Fig. 4(a) illustrates the 2S-PTEQ/FEQ scheme. The number of equalizer coefficients to be estimated is reduced to $2(L_r-1)N_r+(N_t \times N_r)$ per tone. Furthermore the TEQ coefficients $\mathbf{v}_{a(J)}$, $\mathbf{v}_{b(J)}$ and as a result the corresponding PTEQ coefficients depend only on the slowly varying receiver IQ imbalance parameters. This implies that once $\tilde{\mathbf{v}}_{a(J)}$ and $\tilde{\mathbf{v}}_{b(J)}$ are accurately known from Eq. (19), further channel variations require the re-estimation of only the $\mathbf{W}_{a(J,K)}[l]$ coefficients. This results in an overall lower computational complexity as well as a lower training overhead requirement of only $M_{lb} \geq N_r$.

Note:

- *Residual CFO error correction*: In Eq. (19), the TEQ coefficients may not be accurately estimated especially if the auto-correlation based CFO estimation scheme is used in the case of large CFOs. This is because the accuracy of the CFO estimation algorithm in turn depends on the amount of IQ imbalance in the received symbol. Thus in order to further improve the estimate $\Delta\tilde{f}$, we now replace $\mathbf{z}_{(J)}^{(i_s)}$ and $\mathbf{z}_{(J)}^{(j_s)}$ in Eq. (8) with the symbol $\mathbf{z}_{q(J)}^{(i_s)}$ and $\mathbf{z}_{q(J)}^{(j_s)}$ obtained after receiver IQ imbalance has been partially compensated in the

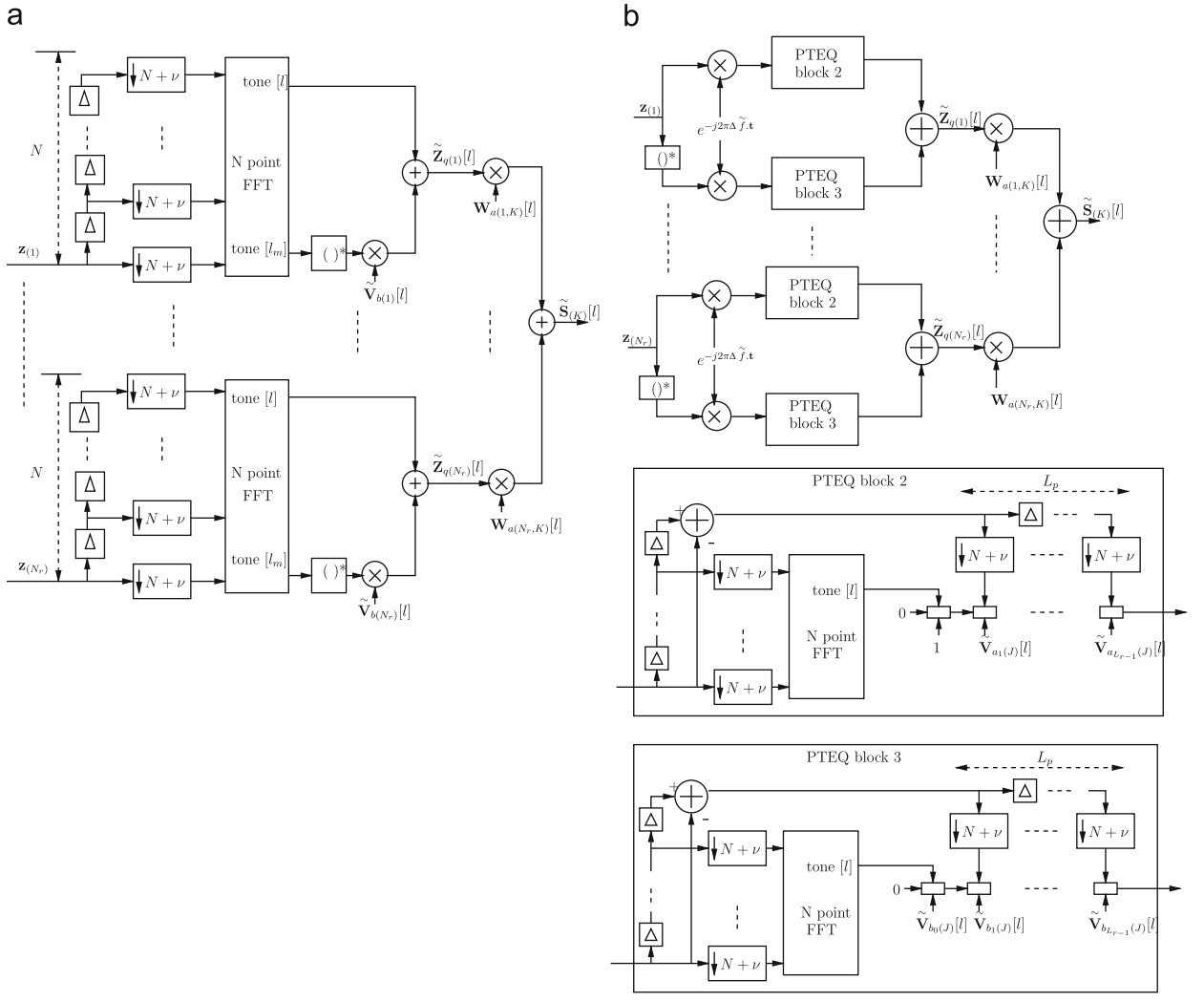


Fig. 4. Decoupled compensation scheme for MIMO OFDM system: (a) system impaired with receiver IQ imbalance and CFO, (b) system impaired with only receiver IQ imbalance.

STS sequence. An expression similar to Eq. (16) can now be written for $\mathbf{z}_{q(J)}^{(i_s)}$ with TEQ estimates obtained from Eq. (19)

$$\mathbf{z}_{q(J)}^{(i_s)} = \mathbf{z}_{(J)}^{(i_s)} \star \widetilde{\mathbf{v}}_{a(J)} + \mathbf{z}_{(J)}^{*(i_s)} \star \widetilde{\mathbf{v}}_{b(J)}$$

$$\begin{bmatrix} \mathbf{z}_{q_1(J)}^{(i_s)} \\ \vdots \\ \mathbf{z}_{q_{N_s}(J)}^{(i_s)} \end{bmatrix} = \left[\begin{array}{cccc} \mathbf{z}_{1(J)}^{(i_s)} & \mathbf{z}_{N_s(J)}^{(i_s-1)} & \cdots & \mathbf{z}_{N_s-L_r+2(J)}^{(i_s-1)} \\ \multicolumn{4}{c}{\vdots} \\ \mathbf{z}_{N_s(J)}^{(i_s)} & \mathbf{z}_{N_s-1(J)}^{(i_s)} & \cdots & \mathbf{z}_{N_s-L_r+1(J)}^{(i_s)} \end{array}\right] \begin{bmatrix} 1 \\ \widetilde{\mathbf{v}}_{a_1(J)} \\ \vdots \\ \widetilde{\mathbf{v}}_{a_{L_r-1}(J)} \end{bmatrix} + \left[\begin{array}{cccc} \mathbf{z}_{1(J)}^{*(i_s)} & \mathbf{z}_{N_s(J)}^{*(i_s-1)} & \cdots & \mathbf{z}_{N_s-L_r+2(J)}^{*(i_s-1)} \\ \multicolumn{4}{c}{\vdots} \\ \mathbf{z}_{N_s(J)}^{*(i_s)} & \mathbf{z}_{N_s-1(J)}^{*(i_s)} & \cdots & \mathbf{z}_{N_s-L_r+1(J)}^{*(i_s)} \end{array}\right] \begin{bmatrix} \widetilde{\mathbf{v}}_{b_0(J)} \\ \widetilde{\mathbf{v}}_{b_1(J)} \\ \vdots \\ \widetilde{\mathbf{v}}_{b_{L_r-1}(J)} \end{bmatrix} \tag{21}$$

where i_s=2…M_s. This time the CFO estimation algorithm (8) provides a much finer estimate as the receiver IQ imbalance has been partially compensated. Eqs. (16)–(19) are then followed so as to obtain an improved estimate of the filter coefficients. Thus we can repeat the entire set of Eqs. (8) and (16)–(19) a number of times until sufficiently accurate estimates of both $\Delta\tilde{f}$ and $\tilde{\mathbf{v}}_{ab(J)}$ are available.

3.2.2. Receiver IQ imbalance compensation

The 2S-PTEQ/FEQ scheme proposed here is applicable irrespective of the amount of CFO in the communication model, hence it is also applicable when there in no CFO. However, it is possible to derive a more efficient and a low cost de-coupled based solution when there is only receiver IQ imbalance. The de-coupled scheme in this case is further simplified by directly estimating the compensation coefficients for receiver IQ imbalance in the frequency domain.

In the case of only receiver IQ imbalance, we can write the received symbol (Eq. (6)) and the complex conjugate of its mirror symbol as follows:

$$\mathbf{Z}_{(J)}[l] = [\mathbf{G}_{ra(J)}[l] \;\; \mathbf{G}_{rb(J)}[l]] \begin{bmatrix} \sum_{K=1}^{N_t} \mathbf{H}_{(J,K)}[l] \cdot \mathbf{S}_{(K)}[l] + \mathbf{N}_{(J)}[l] \\ \sum_{K=1}^{N_t} \mathbf{H}_{(J,K)}^{*}[l_m] \cdot \mathbf{S}_{(K)}^{*}[l_m] + \mathbf{N}_{(J)}^{*}[l_m] \end{bmatrix}$$

$$\mathbf{Z}_{(J)}^{*}[l_m] = [\mathbf{G}_{rb(J)}^{*}[l_m] \;\; \mathbf{G}_{ra(J)}^{*}[l_m]] \begin{bmatrix} \sum_{K=1}^{N_t} \mathbf{H}_{(J,K)}[l] \cdot \mathbf{S}_{(K)}[l] + \mathbf{N}_{(J)}[l] \\ \sum_{K=1}^{N_t} \mathbf{H}_{(J,K)}^{*}[l_m] \cdot \mathbf{S}_{(K)}^{*}[l_m] + \mathbf{N}_{(J)}^{*}[l_m] \end{bmatrix} \tag{22}$$

A first stage FEQ may then be applied that combines $\mathbf{Z}_{(J)}[l]$ and $\mathbf{Z}_{(J)}^{*}[l_m]$ as follows:

$$\tilde{\mathbf{Z}}_{q(J)}[l] = [1 \;\; \mathbf{V}_{b(J)}[l]] \begin{bmatrix} \mathbf{Z}_{(J)}[l] \\ \mathbf{Z}_{(J)}^{*}[l_m] \end{bmatrix} = [1 \;\; \mathbf{V}_{b(J)}[l]] \begin{bmatrix} \mathbf{G}_{ra(J)}[l] & \mathbf{G}_{rb(J)}[l] \\ \mathbf{G}_{rb(J)}^{*}[l_m] & \mathbf{G}_{ra(J)}^{*}[l_m] \end{bmatrix} \times \begin{bmatrix} \sum_{K=1}^{N_t} \mathbf{H}_{(J,K)}[l] \cdot \mathbf{S}_{(K)}[l] + \mathbf{N}_{(J)}[l] \\ \sum_{K=1}^{N_t} \mathbf{H}_{(J,K)}^{*}[l_m] \cdot \mathbf{S}_{(K)}^{*}[l_m] + \mathbf{N}_{(J)}^{*}[l_m] \end{bmatrix} \tag{23}$$

In Eq. (23), the interference terms from the mirror tones $\sum_{K=1}^{N_t} \mathbf{H}_{(J,K)}^{*}[l_m] \cdot \mathbf{S}_{(K)}^{*}[l_m] + \mathbf{N}_{(J)}^{*}[l_m]$ vanish if the filter coefficient $\mathbf{V}_{b(J)}[l]$ is equal to

$$\mathbf{V}_{b(J)}[l] = -\frac{\mathbf{G}_{rb(J)}[l]}{\mathbf{G}_{ra(J)}^{*}[l_m]} \tag{24}$$

Finally Eq. (23) can be re-written as

$$\tilde{\mathbf{Z}}_{q(J)}[l] = \mathbf{G}_{x(J)}[l] \sum_{K=1}^{N_t} \mathbf{H}_{(J,K)}[l] \cdot \mathbf{S}_{(K)}[l] + \mathbf{G}_{x(J)}[l] \mathbf{N}_{(J)}[l] \tag{25}$$

where the scaling term

$$\mathbf{G}_{x(J)}[l] = \left[\mathbf{G}_{ra(J)}[l] - \frac{\mathbf{G}_{rb(J)}[l] \cdot \mathbf{G}_{rb_m(J)}^{*}[l_m]}{\mathbf{G}_{ra_m(J)}^{*}[l_m]} \right]$$

is considered as part of the channel. It should be noted that the coefficient $\mathbf{V}_{b(J)}[l]$ equally compensates for the interference terms from the mirror tones in the noise $\mathbf{N}_{(J)}^{*}[l_m]$ along with the received OFDM symbols $\sum_{K=1}^{N_t} \mathbf{H}_{(J,K)}[l] \cdot \mathbf{S}_{(K)}[l]$, and thus there is no noise amplification in the resultant symbol $\tilde{\mathbf{Z}}_{q(J)}[l]$.

To estimate the FEQ coefficients in Eq. (23), we consider the same sequence of M_{la} phase rotated LTSs as explained in Section 3.2.1. Now Eq. (23) can be written for the lth tone of the ith LTS as follows:

$$\tilde{\mathbf{Z}}_{q(J)}^{(i)}[l] = [1 \;\; \mathbf{V}_{b(J)}[l]] \begin{bmatrix} \mathbf{G}_{ra(J)}[l] & \mathbf{G}_{rb(J)}[l] \\ \mathbf{G}_{rb_m(J)}^{*}[l] & \mathbf{G}_{ra_m(J)}^{*}[l] \end{bmatrix}$$

$$\times \begin{bmatrix} \sum_{K=1}^{N_t} e^{j\Phi^{(i)}} \mathbf{H}_{(J,K)}[l] \cdot \mathbf{S}_{(K)}[l] + \tilde{\mathbf{N}}_{(J)}^{(i)}[l] \\ \sum_{K=1}^{N_t} e^{-j\Phi^{(i)}} \mathbf{H}_{(J,K)}^{*}[l_m] \cdot \mathbf{S}_{(K)}^{*}[l_m] + \tilde{\mathbf{N}}_{(J)}^{*(i)}[l_m] \end{bmatrix} \quad (26)$$

Thus in the noiseless case, we can relate pairs of received symbols as follows:

$$\tilde{\mathbf{Z}}_{q(J)}^{(j)}[l] = e^{j\Omega} \tilde{\mathbf{Z}}_{q(J)}^{(i)}[l]$$

$$\mathbf{Z}_{(J)}^{(j)}[l] - e^{j\Omega} \mathbf{Z}_{(J)}^{(i)}[l] = (e^{j\Omega} \mathbf{Z}_{(J)}^{*(i)}[l_m] - \mathbf{Z}_{(J)}^{*(j)}[l_m]) \mathbf{V}_{b(J)}[l] \quad (27)$$

where $\Omega = \Phi^{(j)} - \Phi^{(i)}$, $i = 1 \ldots M_l - 1$, $j = i+1 \ldots M_l$ and $j > i$. In matrix form, Eq. (27) can be written as

$$\underbrace{\begin{bmatrix} \mathbf{Z}_{(J)}^{(2)}[l] - e^{J(\Phi^{(2)} - \Phi^{(1)})} \mathbf{Z}_{(J)}^{(1)}[l] \\ \vdots \\ \mathbf{Z}_{(J)}^{(M_l)}[l] - e^{J(\Phi^{(M_l)} - \Phi^{(1)})} \mathbf{Z}_{(J)}^{(1)}[l] \\ \mathbf{Z}_{(J)}^{(3)}[l] - e^{J(\Phi^{(3)} - \Phi^{(2)})} \mathbf{Z}_{(J)}^{(2)}[l] \\ \vdots \\ \mathbf{Z}_{(J)}^{(M_l)}[l] - e^{J(\Phi^{(M_l)} - \Phi^{(M_l-1)})} \mathbf{Z}_{(J)}^{(M_l-1)}[l] \end{bmatrix}}_{\mathbf{A}_{tot-(J)}[l]} = \underbrace{\begin{bmatrix} (e^{J(\Phi^{(2)} - \Phi^{(1)})} \mathbf{Z}_{(J)}^{*(1)}[l_m] - \mathbf{Z}_{(J)}^{*(2)}[l_m]) \\ \vdots \\ (e^{J(\Phi^{(M_l)} - \Phi^{(1)})} \mathbf{Z}_{(J)}^{*(1)}[l_m] - \mathbf{Z}_{(J)}^{*(M_l)}[l_m]) \\ (e^{J(\Phi^{(3)} - \Phi^{(2)})} \mathbf{Z}_{(J)}^{*(2)}[l_m] - \mathbf{Z}_{(J)}^{*(3)}[l_m]) \\ \vdots \\ (e^{J(\Phi^{(M_l)} - \Phi^{(M_l-1)})} \mathbf{Z}_{(J)}^{*(M_l-1)}[l_m] - \mathbf{Z}_{(J)}^{*(M_l)}[l_m]) \end{bmatrix}}_{\mathbf{B}_{tot-(J)}[l_m]} \mathbf{V}_{b(J)}[l] \quad (28)$$

We can now compute the estimate of FEQ coefficients $\tilde{\mathbf{V}}_{b(J)}[l]$ as

$$\tilde{\mathbf{V}}_{b(J)}[l] = \mathbf{B}_{tot-(J)}^{\dagger}[l_m] \mathbf{A}_{tot-(J)}[l] \quad (29)$$

Assuming that the receiver IQ imbalance has been properly compensated, a standard MIMO equalizer scheme is then applied (Eq. (20)), to estimate the transmitted symbols. We will refer to this two-stage equalization as the **2S-FEQ** scheme. The number of equalizer coefficients to be estimated is $N_r + (N_r \times N_t)$ per tone. Thus in the case of only receiver IQ imbalance, it is preferable to implement the 2S-FEQ scheme instead of the 2S-PTEQ/FEQ scheme. The 2S-FEQ scheme is illustrated in Fig. 4(b). It should be noted that the 2S-PTEQ/FEQ scheme and the 2S-/FEQ scheme, provide different solutions for the compensation of receiver IQ imbalance: the 2S-PTEQ/FEQ scheme is based on estimating the mismatch filter impulse responses while the 2S-FEQ scheme is based on the suppression of interference terms from the mirror tones.

4. Computational complexity

Table 1 summarizes the computational complexity requirement in terms of the number of coefficients to be estimated per tone for different RF front-end scenarios. It can be observed that the de-coupled schemes (formulas (19) and (29)) provide a significant complexity reduction compared to the joint compensation scheme (formula (15)). The joint compensation scheme on the other hand provides a solution that can always straightforwardly be trained for all combinations of RF impairments.

5. Simulations

We consider a system very similar to the MIMO extension of the uncoded IEEE 802.11a standard [18], to evaluate the proposed compensation schemes in the presence of IQ imbalance and CFO. The performance comparison is made with an ideal system with no front-end distortion and with a system with no compensation algorithm included.

The parameters used in the simulation are as follows: the OFDM data symbol and LTS length N=64, the CP length $v = 16$ and STS length N_s=16. The length of the STS sequence M_s=10 while the length of the linearly independent LTS sequence is based on the number of coefficients required for the initialization of PTEQ/FEQ structure for every tone. In the simulations, we have considered the LTS sequence to be twice as long as the number of coefficients required for initialization. In the case of de-coupled schemes, we consider M_{la}=4 phase

Table 1
Computational complexity in terms of the number of coefficients to be estimated per tone.

RF front-end scenario	De-coupled schemes 2S-(PTEQ)/FEQ	Joint scheme PTEQ
FS receiver IQ	$N_r + (N_t \times N_r)$	$2(N_t \times N_r)$
FS transmitter/receiver IQ	–	$2(N_t \times N_r)$
FI receiver IQ + CFO	$N_r + (N_t \times N_r)$	$2(N_t \times N_r)$
FS receiver IQ + CFO	$(2L_r - 1)N_r + (N_t \times N_r)$	$2L_r(N_t \times N_r)$
FI transmitter/receiver IQ + CFO	–	$4(N_t \times N_r)$
FS transmitter/receiver IQ + CFO	–	$4L_r(N_t \times N_r)$

rotated LTS sequence to estimate the coefficients for the compensation of receiver IQ imbalance. The phase rotations of the LTS are then given as $\phi_l = 0,\ \pi/4,\ \pi/2$ and $3\pi/2$. The multipath channel has length L=4 taps. The taps of the multipath channel are chosen independently with complex Gaussian distribution. The transmitter/receiver front-end mismatched filter impulse responses are $\mathbf{h}_{ti(K)} = \mathbf{h}_{ri(J)} = [0.1\ 0.5\ 0.06]$ and $\mathbf{h}_{tq(K)} = \mathbf{h}_{rq(J)} = [0.06\ 0.5\ 0.1]$, the FI amplitude imbalances are $g_{t(K)} = g_{r(J)} = 5\%$ and the phase imbalances are $\phi_{t(K)} = \phi_{r(J)} = 5^{\circ}$. The same IQ imbalance values have been kept across all antenna branches so as to keep the simulation process simple. We have considered imbalance levels higher than those observed in a practical receiver. However, we consider such an extreme case to evaluate the robustness/effectiveness of the proposed compensation schemes. All the bit-error-rate (BER) results depicted are obtained by averaging the BER curves over 10^4 independent channel realizations.

Fig. 5 shows the performance of the two CFO estimation algorithms: the auto-correlation based scheme [7], the NLS based scheme [10], used for 16QAM 2×2 MIMO system. The proposed iterative auto-correlation based scheme applicable only in the case of 2S-PTEQ/FEQ is also plotted. In the case of PTEQ based joint compensation scheme, we consider a threshold to decide between the two non-iterative CFO estimation schemes. The performance curves are obtained at 40 dB signal-to-noise ratio (SNR). The figure shows that for the given IQ imbalance values, a good choice for the threshold between the non-iterative CFO estimation schemes will be $\zeta = -0.02$ and $+0.02$ where ζ is the ratio of the actual CFO Δf and the tone spacing $1/T \cdot N$, i.e. $\zeta = \Delta f \cdot T \cdot N$. For smaller IQ imbalance values, the performance of the two estimation schemes will be further improved. In the NLS scheme, we have used a step size of $\Delta\zeta = 0.0005$ for the exhaustive search. The figure shows that for the non-iterative based auto-correlation scheme, the performance deteriorates as the CFO is increased from $\zeta = 0$ to ± 0.5. The NLS scheme shows an inverse characteristic with poorest performance at $\zeta = 0$ and a gradual improvement as the CFO is increased to $\zeta = \pm 0.1$. The mean-square-error (MSE) for the NLS scheme saturates after $\zeta = \pm 0.1$. The proposed iterative scheme shows an improved performance as the number of iterations is increased, i.e. from 2 to 3. The iterative scheme is robust and good estimates are obtained for the entire range of CFO values. The CFO error correction for the PTEQ scheme is explained in the next figure.

Fig. 6(a) and (b), shows the performance curves obtained for an uncoded 64QAM 2×2 uncoded MIMO OFDM system with a PTEQ based joint compensation scheme. A training based RLS algorithm is used to initialize the PTEQ coefficients. This is because the RLS scheme provides an optimal convergence and achieves initialization with an acceptably small number of training symbols. In Fig. 6(a), we search for an optimal CFO value $\tilde{\zeta} = \Delta\tilde{f} \cdot T \cdot N$ together with optimal PTEQ coefficients. We have considered a fixed $\zeta = 0.32$ in the system. The figure shows the MSE obtained with the LTS sequence for various residual CFO estimation

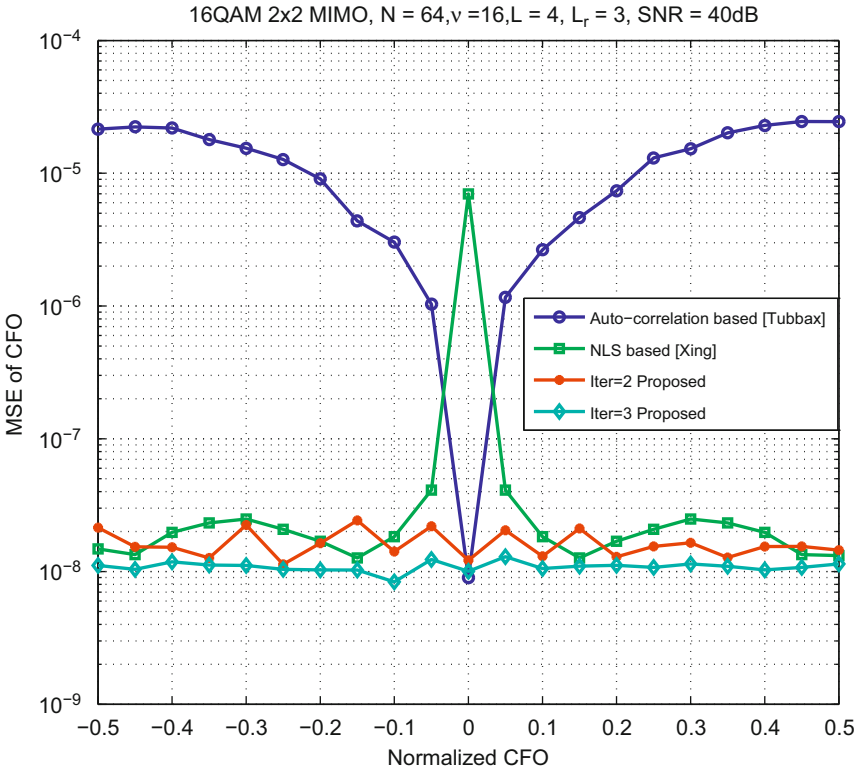


Fig. 5. MSE observed in the estimation of CFO in the presence of receiver IQ imbalance.

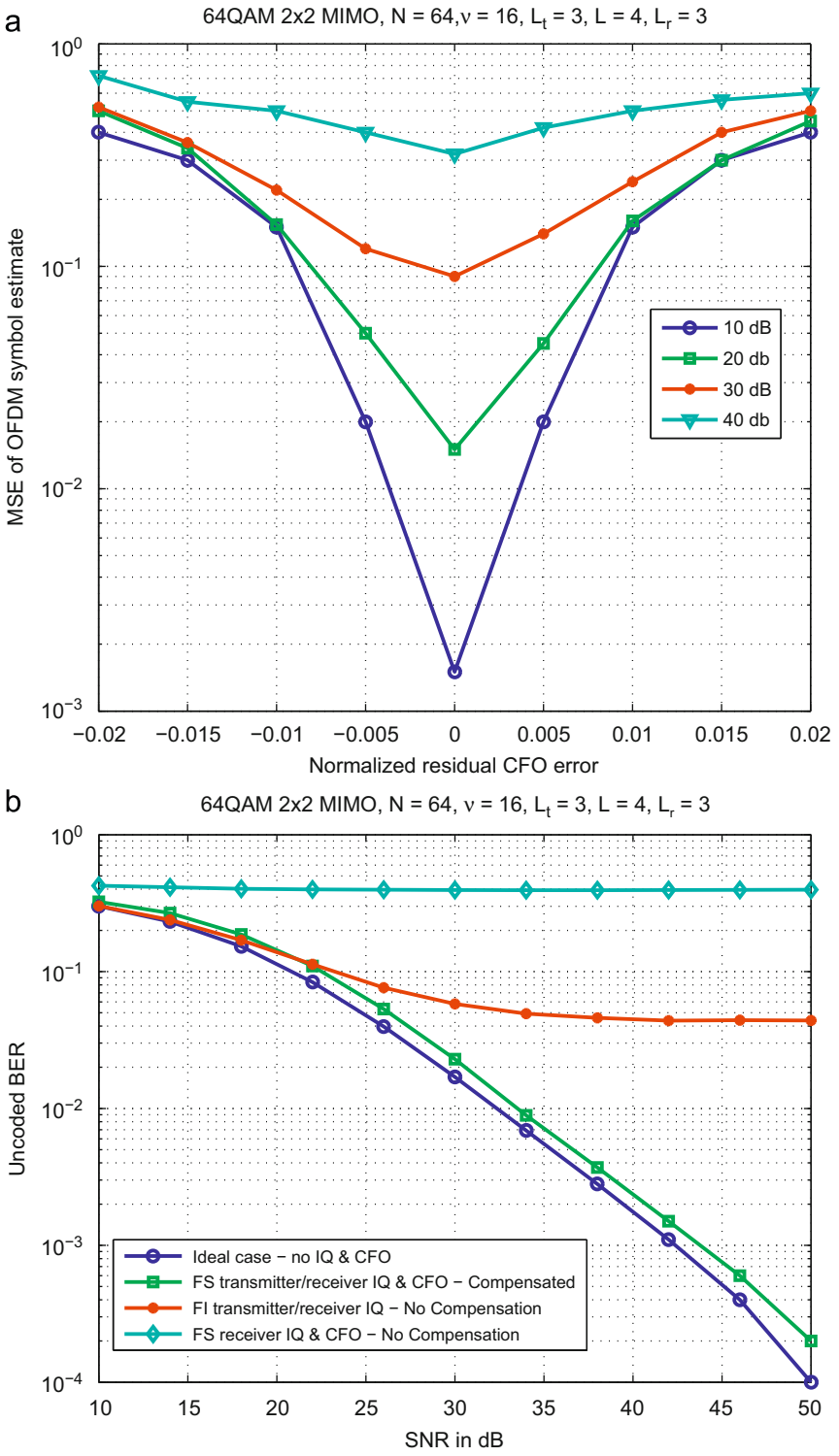


Fig. 6. Performance results with PTEQ based compensation scheme for a system impaired with transmitter/receiver IQ imbalance and CFO. (a) Shows the MSE obtained with the LTS sequence for various residual CFO estimation errors. A fixed $\zeta = 0.32$ is considered in the simulation. (b) Shows the BER vs SNR curves obtained for the PTEQ scheme. We consider CFOs uniformly distributed between $\zeta = [-0.2 \leftrightarrow 0.2]$ for every channel realization considered in the simulation.

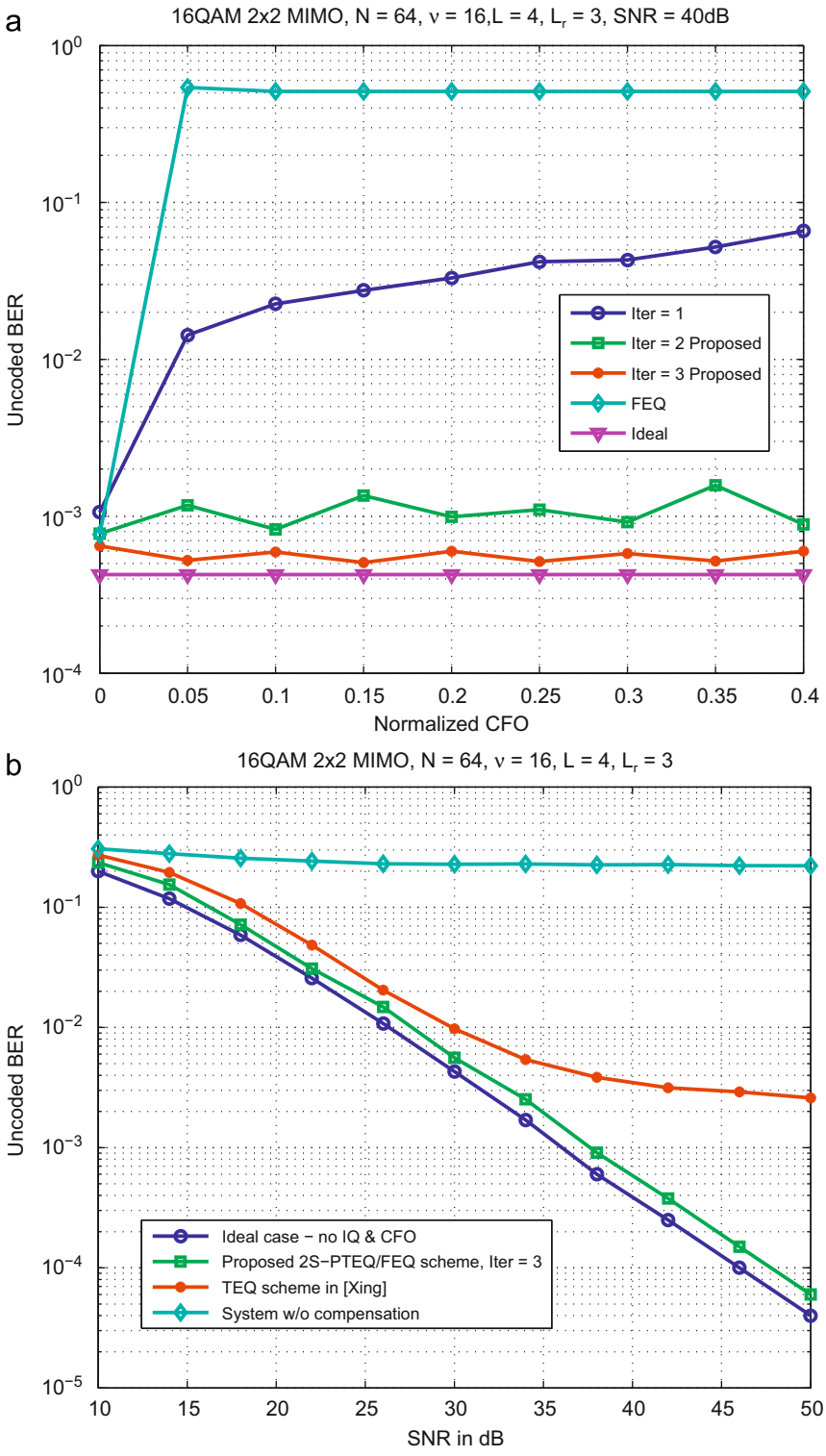


Fig. 7. Performance results with 2S-PTEQ/FEQ based compensation scheme for a system impaired with receiver IQ imbalance and CFO: (a) BER vs normalized CFO, (b) BER vs SNR.

errors $e_\zeta = \zeta - \tilde{\zeta}$. It can be seen that for an accurate estimate of the CFO, i.e. ($\tilde{\zeta} = \zeta$), the MSE reaches a minimum. There is a big dip in MSE and this becomes even more prominent as the SNR is increased from 10 to 40 dB. This shows that a significant improvement in performance can be obtained for a good CFO estimate and that the search for an accurate CFO

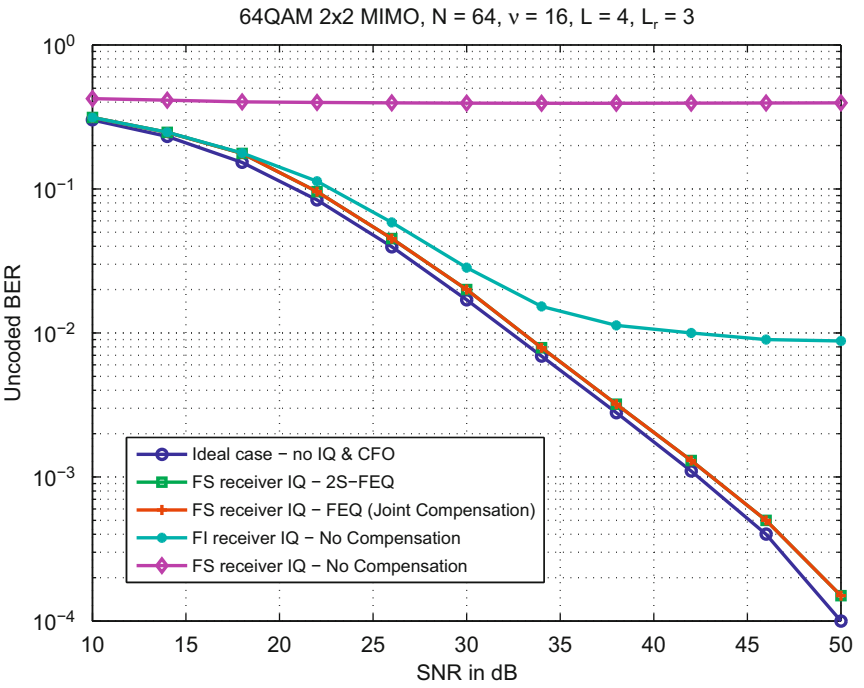


Fig. 8. BER vs SNR for a system impaired with only receiver IQ imbalance.

estimate becomes easier at higher SNR values. The PTEQ coefficients obtained for this resulting CFO estimate $\tilde{\zeta}$ are then used for equalization. Fig. 6(b) shows the BER vs SNR curves obtained for the PTEQ scheme. We consider CFOs uniformly distributed between $\zeta = [-0.2 \leftrightarrow 0.2]$ for every channel realization considered in the simulation. In the presence of FS transmitter/receiver IQ imbalance and CFO with no compensation scheme in place, the system is completely unusable. Even for the case when there is only FI transmitter/receiver IQ imbalance, the BER is very high. With the compensation scheme in place, the performance is very close to the ideal case. For low SNR, it may be difficult to accurately determine the CFO and hence the performance is poor compared to the system with no CFO and also no compensation scheme in place. The compensation performance is seen to depend on how accurately the equalizer coefficients can converge to the optimal values.

Fig. 7(a) and (b) shows the BER performance against the normalized CFO and SNR for the 2S-PTEQ/FEQ based compensation scheme in a 16QAM 2×2 uncoded MIMO system. In Fig. 7(a), the BER performance is also plotted for a FEQ, Eq. (11), that considers the joint compensation of only transmitter/receiver IQ imbalance in the communication model. The FEQ does not compensate for CFO distortions. It can be observed that for $\zeta = 0$, the FEQ scheme and the 2S-PTEQ/FEQ scheme provide good compensation. But as ζ is increased, the performance of the FEQ and the 2S-PTEQ/FEQ with only one iteration deteriorates. The 2S-PTEQ/FEQ scheme shows poor performance as the CFO estimate may not be accurate in the first iteration. As we perform more iterations, the CFO and receiver IQ imbalance estimates become more accurate resulting in improved BER performance. For the given IQ imbalance and CFO values, the proposed scheme requires only three iterations to obtain good performance. Fig. 7(b) shows the BER vs SNR for a system with only receiver IQ imbalance and CFO. Here, we consider a CFO $\zeta = 0.32$. The proposed compensation scheme is compared with the one in [10] and with the system with no compensation scheme in place. It is seen that with no compensation scheme in place, the system is completely unusable and thus a digital compensation scheme is necessary. The proposed scheme in [10] gives poor performance at higher SNR. This is because the compensation scheme depends on only one filter that measures the difference in impulse response of two branch filters. A filter of this kind exhibits infinite impulse response and may also require the addition of cyclic postfix samples to the OFDM symbols [13]. The proposed compensation scheme estimates the complete impulse response of the two branch filters $\mathbf{v}_{a(J)}$ and $\mathbf{v}_{b(J)}$ resulting in improved performance. The performance is further improved by performing multiple iterations over the CFO and IQ imbalance estimation.

Fig. 8 shows the performance curves (BER vs SNR) in the presence of only receiver IQ imbalance in a 64QAM 2×2 uncoded MIMO OFDM system. The BER results show that the 2S-FEQ scheme performs very well and the results are similar to the FEQ based joint compensation scheme in (11) and [14–16]. Given the availability of adequate training sequence, the joint compensation scheme and the de-coupled scheme provide the same system performance. In the de-coupled scheme, once the

first stage of FEQ is initialized, this stage remains fixed and only the second stage of the equalizer is trained for variations in the channel.

6. Conclusion

In this paper we have developed a digital compensation scheme for joint transmitter/receiver frequency selective IQ imbalance, CFO and channel distortion. We have shown that in the case where there is no transmitter IQ imbalance, the receiver IQ imbalance compensation can be de-coupled from the channel equalization resulting in a compensation in two stages. The two-stage scheme results in an overall lower computational requirement. The various compensation schemes are demonstrated to provide a performance close to the ideal case without RF impairments.

References

[1] J. Bingham, Multi-carrier modulation for data transmission: an idea whose time has come, IEEE Communications Magazine (May 1990) 5–14.
[2] G. Stuber, J. Barry, S. Mclaughlin, Y. Li, M. Ingram, T. Pratt, Broadband MIMO-OFDM wireless communications, Proceedings of the IEEE 92 (2) (February 2004) 271–294.
[3] B. Razavi, Design considerations for direct-conversion receivers, IEEE Transactions on Circuits and Systems 44 (6) (June 1997) 428–435.
[4] T. Pollet, M. Van Bladel, M. Moeneclaey, BER sensitivity of OFDM systems to carrier frequency offset and Wiener phase noise, IEEE Transactions on Communications 43 (2/3/4) (1995) 191–193.
[5] M. Valkama, M. Renfors, V. Koivunen, Compensation of frequency-selective IQ imbalances in wideband receivers: models and algorithms, in: Proceedings of the IEEE Third SPAWC workshop, Taoyuan, Taiwan, March 2001, pp. 42–45.
[6] I. Barhumi, M. Moonen, IQ-imbalance compensation for OFDM in the presence of IBI and carrier-frequency offset, IEEE Transactions on Signal Processing 55 (1) (2007) 256–266.
[7] J. Tubbax, B. Come, L. Van der Perre, M. Engels, M. Moonen, H. De Man, Joint compensation of IQ imbalance and carrier frequency offset in OFDM systems, in: Proceedings of the Radio and Wireless Conference, Boston, MA, August 2003, pp. 39–42.
[8] S. Fouladifard, H. Shafiee, Frequency offset estimation in OFDM systems in presence of IQ imbalance, in: Proceedings of the IEEE ICC, Anchorage, AK, May 2003, pp. 2071–2075.
[9] F. Horlin, A. Bourdoux, L. Van der Perre, Low-complexity EM-based joint acquisition of the carrier frequency offset and IQ imbalance, IEEE Transactions on Wireless Communications 7 (2008) 2212–2220.
[10] G. Xing, M. Shen, H. Liu, Frequency offset and I/Q imbalance compensation for direct-conversion receivers, IEEE Transactions on Wireless Communications 4 (2) (March 2005) 673–680.
[11] H. Lin, X. Zhu, K. Yamashita, Pilot-aided low-complexity CFO and I/Q imbalance compensation for OFDM systems, in: Proceedings of IEEE ICC 2008, Beijing, China, May 2008, pp. 1–5.
[12] D. Tandur, M. Moonen, Joint compensation of OFDM frequency selective transmitter/receiver IQ imbalance, Eurasip Journal on Wireless Communications and Networking (JWCN) 2007 (2) (2007) (10pp, Article ID 68563).
[13] D. Tandur, C. Lee, M. Moonen, Efficient compensation of RF impairments for OFDM systems, in: Proceedings of IEEE Wireless Communications and Networking Conference (WCNC), Budapest, Hungary, April 2009.
[14] A. Tarighat, A.H. Sayed, MIMO OFDM receivers for systems with IQ imbalances, IEEE Transactions on Signal Processing 53 (9) (September 2005) 3583–3596.
[15] R.M. Rao, B. Daneshrad, I/Q mismatch cancellation for MIMO-OFDM systems, in: Proceedings of the IEEE International Symposium on Personal, Indoor, Mobile Radio Communications (PIMRC), September 2004, vol. 5, pp. 2710–2714.
[16] T. Schenck, P. Smulders, E. Fledderus, Estimation and compensation of frequency selective transmitter/receiver IQ imbalance in MIMO OFDM systems, in: Proceedings of IEEE ICC, Istanbul, Turkey, June 2006, pp. 251–256.
[17] D. Tandur, M. Moonen, Compensation of RF impairments in MIMO OFDM systems, in: Proceedings of IEEE International Conference on Acoustics, Speech and Signal Processing (ICASSP), Las Vegas, Nevada, April 2008, pp. 3097–3100.
[18] IEEE Standard 802.11a-1999, Wireless LAN medium access control (MAC) and physical layer (PHY) specifications, high-speed physical layer in the 5 GHz band, 1999.
[19] C. Muschallik, Influence of RF oscillators on an OFDM signal, IEEE Transactions on Consumer Electronics 41 (3) (August 1995) 592–603.
[20] F.D. Neeser, J.L. Massey, Proper complex random processes with applications to information theory, IEEE Transactions on Information Theory 39 (4) (July 1993) 1293–1302.
[21] K. van Acker, G. Leus, M. Moonen, Per-tone equalization for DMT based systems, IEEE Transactions on Communications 49 (1) (January 2001).